HHS Public Access

Author manuscript

Glia. Author manuscript; available in PMC 2021 December 22.

Published in final edited form as:

Glia. 2020 February ; 68(2): 263–279. doi:10.1002/glia.23715.

A Modified Flavonoid Accelerates Oligodendrocyte Maturation and Functional Remyelination

Weiping Su[1], **Steven Matsumoto**[1,2], **Fatima Banine**[1], **Taasin Srivastava**[3], **Justin Dean**[4], **Scott Foster**[1], **Peter Pham**[1], **Brian Hammond**[1], **Alec Peters**[1], **Kesturu S. Girish**[5], **Kanchugarakoppal. S. Rangappa**[6], **Salundi Basappa**[7], **Joachim Jose**[8], **Jon D. Hennebold**[9], **Melinda J. Murphy**[9], **Jill Bennett-Toomey**[9], **Stephen A. Back**[3,10], **Larry S. Sherman**[1,11]

[1]Division of Neuroscience, Oregon National Primate Research Center, Oregon Health & Science University, USA

[2]Integrative Biosciences Department, School Dentistry, Oregon Health & Science University, USA

[3]Department of Pediatrics, Oregon Health & Science University, USA

[4]Department of Physiology, Faculty of Medical and Health Sciences, University of Auckland, New Zealand

[5]Department of Studies and Research in Biochemistry, Tumkur University, Tumakuru, India

[6]Institute of Excellence, Vijnana Bhavan, University of Mysore, Manasagangotri, Mysuru, India

[7]Department of Studies in Organic Chemistry, University of Mysore, Manasagangotri, Mysuru, India

[8]Institute of Pharmaceutical and Medicinal Chemistry, Phytochemistry, PharmaCampus, Westfälische Wilhelms-Universität Münster, Münster, Germany

[9]Division of Reproductive & Developmental Sciences, Oregon National Primate Research Center, Oregon Health & Science University, USA

[10]Department of Neurology, Oregon Health & Science University, USA

[11]Department of Cell, Developmental and Cancer Biology, Oregon Health & Science University, USA

Abstract

Myelination delay and remyelination failure following insults to the central nervous system (CNS) impede axonal conduction and lead to motor, sensory and cognitive impairments. Both myelination and remyelination are often inhibited or delayed due to the failure of oligodendrocyte progenitor cells (OPCs) to mature into myelinating oligodendrocytes (OLs). Digestion products of the glycosaminoglycan hyaluronan (HA) have been implicated in blocking OPC maturation, but how these digestion products are generated is unclear. We tested the possibility that hyaluronidase

Correspondence: Larry S. Sherman, Division of Neuroscience, Oregon National Primate Research Center, Oregon Health & Science University, 505 NW 185th Avenue, Beaverton, OR 97006 USA, shermanl@ohsu.edu.

CONFLICT OF INTERESTS

The authors declare that they have no competing interests

activity is directly linked to the inhibition of OPC maturation by developing a novel modified flavonoid that functions as a hyaluronidase inhibitor. This compound, called S3, blocks some but not all hyaluronidases and only inhibits matrix metalloproteinase activity at high concentrations. We find that S3 reverses HA-mediated inhibition of OPC maturation *in vitro*, an effect that can be overcome by excess recombinant hyaluronidase. Furthermore, we find that hyaluronidase inhibition by S3 accelerates OPC maturation in an *in vitro* model of perinatal white matter injury. Finally, blocking hyaluronidase activity with S3 promotes functional remyelination in mice with lysolecithin-induced demyelinating corpus callosum lesions. All together, these findings support the notion that hyaluronidase activity originating from OPCs in CNS lesions is sufficient to prevent OPC maturation, which delays myelination or blocks remyelination. These data also indicate that modified flavonoids can act as selective inhibitors of hyaluronidase activity and can promote OPC maturation, making them excellent candidates to accelerate myelination or promote remyelination following perinatal and adult CNS insults.

Keywords

Myelin; oligodendrocyte; hyaluronan; hyaluronidase; flavonoid

1. INTRODUCTION

Myelination delay and remyelination failure occur following a number of insults to the central nervous system (CNS) including perinatal hypoxia-ischemia (Back and Rosenberg, 2014) and autoimmune attacks such as those that occur in patients with multiple sclerosis (MS; Lassmann, 2014; Stangel et al., 2017). While axonal damage can account for some myelination and remyelination deficits, there is growing evidence that CNS myelination deficits in the perinatal and adult brain are linked to the failure of oligodendrocyte progenitor cells (OPCs) to mature into myelin forming oligodendrocytes (OLs; Franklin and ffrench-Constant, 2017). Indeed, a number of studies have demonstrated the potential efficacy of promoting OPC maturation as a strategy to promote remyelination (Cole et al., 2017). Thus, identifying the mechanisms underlying the inhibition of OPC maturation would provide novel targets for therapies aimed at accelerating myelination or remyelination.

We and others have demonstrated that high molecular weight (HMW) forms of the glycosaminoglycan hyaluronan (HA) accumulate in demyelinating MS lesions (Back et al., 2005; Sloane et al., 2010), in the white matter of infants with periventricular white matter injury (Buser et al., 2012), following traumatic CNS injury (Struve et al., 2005; Xing et al., 2013), in vanishing white matter disease (Bugiani et al., 2013), in individuals with vascular cognitive impairment (Back et al., 2011), and during the course of normative brain aging (Suzuki et al., 1965; Jenkins and Bachelard, 1988; Cargill et al., 2012; Reed et al., 2017). HA accumulation is associated with astrogliosis and the accumulation of OPCs that fail to mature into myelinating OLs in chronic demyelinated lesions (Back et al., 2005; Segovia et al., 2008; Sloane et al., 2010; Back et al., 2011; Riddle et al., 2011; Buser et al., 2012; Bugiani et al., 2013), suggesting that HA disrupts remyelination by preventing OPC maturation (Sherman et al., 2015).

HA is synthesized in mammals by transmembrane hyaluronan synthases (HAS1–3) and catabolized by hyaluronidases that depolymerize HA. The function and expression of different hyaluronidases in the CNS is not well understood. Early studies identified hyaluronidase activity in both gray and white matter (Margolis et al., 1972) that is highly regulated during embryonic CNS development (Polansky et al., 1974). As different hyaluronidase genes were characterized, their expression in the CNS has been controversial. For example, Hyal2 was originally described as absent from the brain (Strobl et al., 1998) while later studies indicated that Hyal2 is expressed by at least some CNS cell types including astrocytes, OL-lineage cells, and brain endothelial cells (Sloane et al., 2010; Lindwall et al., 2013; Preston et al., 2013; Chowdhury et al., 2016). Other hyaluronidases are also expressed in the CNS including HYAL1 and HYAL3 (Csoka et al., 1998; Triggs-Raine et al., 1999; Sloane et al., 2010; Preston et al., 2013), the recently characterized hyaluronidase transmembrane protein-2 (TMEM2) (Golan et al., 2008; Marques et al., 2016; De Angelis et al., 2017; Yamamoto et al., 2017) and the Cell Migration-Inducing hyaluronan binding Protein (CEMIP) (also called HYBID and KIAA1199), which has been implicated in hippocampal learning and memory (Yoshino et al., 2017). TMEM2 and CEMIP appear to share some features with two other hyaluronidases, PH20 (also called SPAM1) and Hyal5, which are localized to the cell surface, can digest extracellular HA at neutral pH, and have been implicated in fertilization (Reitlinger et al., 2007).

OPCs can digest HA and express multiple hyaluronidases (Sloane et al., 2010; Golan et al., 2008; Preston et al., 2013; Marques et al., 2016). We previously reported that the activities of PH20, Hyal2, and Hyal5 blocked OPC maturation when expressed by OPCs *in vitro*, with PH20 having the greatest inhibitory activity. We also found that digestion products of HA in a specific size range blocked remyelination *in vitro* and *in vivo* (Preston et al., 2013; Srivastava et al., 2018). Hyal5 has not been detected in OPCs or in the CNS (Preston et al, 2013) while PH20 RNA has been reported to only be transiently expressed by OPCs or other cells, especially following CNS insults (Sloane et al., 2010; Preston et al., 2013; Hagen et al., 2014; Xing et al., 2014; Sherman and Back, 2017). However, other reports have failed to find PH20 expression in OPCs or in demyelinating lesions and one study indicated that a pegylated form of recombinant human PH20 failed to influence OPC maturation (Marella et al., 2017; but see Sherman and Back, 2017). In contrast, TMEM-2 has been detected in OL lineage cells (Golan et al., 2008; Marques et al., 2016) and CEMIP is widely expressed in the brain and is elevated in demyelinating lesions (Yoshino et al., 2017; Marella et al, 2018). Thus, while PH20 may be at least transiently elevated in OPCs in demyelinating lesions, other hyaluronidases with similar activities may contribute to myelination delay or remyelination failure.

Since there are multiple cell surface hyaluronidases that could generate HA digestion products that block OPC maturation and remyelination, defining the roles of hyaluronidases in OPCs requires pharmacological approaches that inhibit the activities of each of these enzymes. One of the most potent and best characterized pharmacological inhibitors of hyaluronidase activity is Vcpal (L-Ascorbyl 6-palmitate; also called ascorbate 6-hexadecanoate) which inhibits hyaluronidases through hydrophobic interactions with specific enzyme domains (Botzki et al., 2004). Interestingly, Vcpal promotes OPC maturation *in vitro* (Sloane et al., 2010; Preston et al., 2013) and remyelination in

demyelinating lesions (Preston et al., 2013). However, Vcpal must be used at relatively high concentrations, inhibits multiple hyaluronidases, can function as an anti-oxidant, and also inhibits lipoxygenases (Mohamed et al., 2014) which have been implicated in mediating OL survival following CNS injury (Zhang et al., 2007; Haynes and van Leyen, 2013). It is therefore critical to utilize alternative approaches to test if there is a specific role for hyaluronidases in inhibiting OPC maturation and either myelination or remyelination.

Here, we report that a modified flavonoid potently and selectively inhibits the enzymatic activity of PH20 and CEMIP but not Hyal1 or Hyal2. We find that this novel inhibitor promotes OPC maturation in the presence of HMW HA *in vitro*, and that this effect can be overcome by recombinant PH20. Finally, we show that blocking hyaluronidase activity with this modified flavonoid accelerates OPC maturation in a slice culture model of perinatal white matter injury and promotes functional remyelination in a model of adult demyelination. All together, these data indicate that hyaluronidase activity prevents OPC maturation and blocks myelination or remyelination, and that selective hyaluronidase inhibitors can be used to accelerate myelination or remyelination following CNS injuries.

2. MATERIALS AND METHODS

2.1 Reagents

Modified flavonoids (S1-S6) were synthesized as previously described (Srinivasa et al., 2014). Flavonoids were dissolved in dimethylsulfoxide (DMSO) at a concentration of 10 mM and further diluted to a working concentration of 0.4 to 200 μM for enzyme activity assays or for cell culture. 6-O-Palmitoyl-L-ascorbic acid (Vcpal; Sigma) was dissolved in DMSO at a stock concentration of 100 mM and was diluted to final concentration of 25 μM in all assays. Recombinant bovine SPAM1 (rPH20, 1.5 μg/ml, R&D Systems), Recombinant Human Hyaluronidase HYAL1 (rhHyal1, 6 μg/ml, R&D Systems), recombinant Human protein HYAL2 (rhHyal2, 40 μg/ml, MybioSource), Streptomyces hyaluronidase (StrepH; 7.5U/ml, Sigma), and bovine testicular hyaluronidase (BTH; Sigma, 10–20U/ml) were diluted in pH 3.5 or 4.5 (sodium citrate buffer) or pH 7.0 (phosphate-buffered saline, PBS) sample buffer. HMW HA (1.59×10^6 Da, Lifecore) stock solution (2mg/ml) was prepared in PBS, water, or tissue culture medium. N-(4-fluorobenzyl)-1-benzyl-1H-indole-2-carboxamide and N-(4-chlorobenzyl)-1-(4-fluorobenzyl)-1H-indole-3-carboxamide were dissolved in DMSO and used at concentrations between 1 and 50 μM.

2.2 Analysis of HA digestion products

Flavonoids or vehicle alone were pre-incubated with different concentrations of hyaluronidases or dilutions of transfected cell lysates for 1 hr at 37 °C then HMW HA was added to each mixture at a final concentration of 150 μg/ml and incubated for an additional hour. In live cell cultures, cells were transfected with empty vectors or expression vectors carrying different hyaluronidase cDNAs, then the cell growth medium was replaced with serum-free and phenol red-free DMEM containing 50 μg/ml HMW HA, 4.5g/L D-glucose and glutamine, and 110mg/L sodium pyruvate, and different concentrations of S3. Twenty-four hours later, cell medium was collected, spun at 12k rpm for 10 minutes, and supernatant collected. To deactivate enzymes, samples were incubated in a 100 °C water bath for 30

min. Ten microliters of each sample was mixed with 2 μl of 0.02% Bromophenol Blue loading buffer (Bio-Rad Laboratories) and analyzed by gel electrophoresis using a 0.5% agarose (high-gelling-temperature, Fisher) in Tris–acetate–EDTA buffer (40 mM Tris, 5 mM acetate [CH3COONa], and 0.9 mM EDTA, pH 7.9). Gels were stained using the cationic dye Stains-All (Bio-Rad Laboratories) as previously described (Lee and Cowman, 1994) and then photographed. The distribution and intensity of HA in each lane was determined using ImageJ.

2.3 Analysis of metalloproteinase activities

The effects of different concentrations of S3 on gelatinolytic, caseinolytic, fibrinolytic and fibronogenolytic activity when mixed with 2 μg of *Echis carinatus* venom were determined as previously described (Srinivasa et al., 2014).

2.4 Generation of expression vectors

The *CEMIP* expression vector and control vector were purchased from Origene (*Cemip* (NM_030728) Mouse Tagged ORF Clone; pCMV6-Entry Tagged Cloning Vector). The *Tmem2* mouse cDNA was generated from mouse brain RNA using the SuperScript III One-Step RT-PCR System with Platinum™ Taq DNA Polymerase (Invitrogen) according to the manufacturer's instructions using the following primers: Forward primer: ggggtaccacagggtatcatgtatgccgctggttccagg; Reverse primer: ccgctcgagccaagtctctaaagcactttc. The *Tmem2* PCR product was digested with KpnI and XbaI, purified and cloned in pcDNA3.

2.5 Cell Culture

All animal experiments were approved by the Institutional Animal Care and Use Committee at the Oregon Health and Science University. OPCs were prepared from neural stem cells isolated from the medial and lateral ganglionic eminences of embryonic day 13.5 mouse (C57BL/6) embryos and expanded in epidermal growth factor and fibroblast growth factor-2 (both at 10 ng/ml) as neurospheres for one week as previously described (Preston et al., 2013). Neurospheres were dissociated into single cells in trypsin (0.05%, InVitrogen), washed in Dulbecco's Modified Eagle Medium (DMEM) plus 10% fetal bovine serum and plated at 5×10^6 cells/ml on uncoated polystyrene plates in DMEM/F12 media containing 0.1% bovine serum albumin, platelet-derived growth factor (PDGF) AA and fibroblast growth factor-2 at 20 ng/ml each, B27 supplement minus vitamin A (GIBCO), N1 supplement (Sigma) and D-Biotin (10 nM, Sigma) (OPC medium). Small adherent oligospheres formed and were passaged once a week after dissociation with Accutase (Invitrogen). After 2–3 weeks oligospheres were transferred to poly-L-ornithine-coated 100 mm dishes. After 1–2 passages, highly enriched populations (>95%) of PDGFRα+Olig2+O4−OPCs (as assayed by immunocytochemistry) were obtained and further propagated for *in vitro* experiments. For maturation experiments, OPCs were plated at $4–5 \times 10^4$ cells per coverslip and differentiated in DMEM/F12, 0.1% BSA, plus triiodothyronine (T3, 30 nM, Sigma) and N-acetyl-L-cysteine (NAC, Sigma) as previously described (Preston et al., 2013).

HEK293T cells were transfected with expression vectors carrying cDNAs for mouse PH20, Hyal1, Hyal2, or empty vector (constructs described above and previously in Preston et al., 2013), using calcium phosphate precipitate, and CEMIP or Tmem2 (constructs described above) using 2 μg of plasmid for every 1.2×10^6 cells and using Fugene HD (1:3 ratio of DNA:reagent). Forty-eight hours after transfection, cells were washed with PBS, then harvested (for the Hyal1, Hyal2 TMEM2 and PH20 constructs) and suspended in lysis buffer (100mM Na Citrate, 100mM NaCl), while conditioned media were harvested as described in section 2.2 for CEMIP cultures.

2.6 Controlled Ovarian Stimulation (COS) and Oocyte Collection

COS protocols were performed on regularly cycling female rhesus macaques as previously described (Wolf et al., 1989; Hanna et al., 2015). In brief, on day 1 to 4 of menses, monkeys received recombinant human (rh) follicle stimulating hormone (FSH; 30 IUs, IM, twice a day) for 6 days. FSH and rh-luteinizing hormone (LH) were given the next two days (30 IUs each, IM, twice a day). FSH and LH were provided by Merck & Co. and Merck Serono, respectively. To prevent a spontaneous LH surge, a GnRH antagonist, Antide (1 mg/kg, SQ; Salk Institute for Biological Studies) was given when estradiol (E2) levels reached ~ 150 pg/ml. To induce ovulatory events, human chorionic gonadotropin (hCG; 1000 IUs, IM; Novarel, Ferring Pharmaceuticals) was given on day 8 of the protocol. Cumulus-oocyte complexes were aspirated and collected from large antral follicles by laparoscopy 36 hours after hCG administration.

2.7 Hyaluronidase Inhibitor Effects on *In Vitro* Fertilization Rates

Cumulus-oocyte isolation and *in vitro* fertilization (IVF) were described previously (Wolf et al., 1990; Hanna et al., 2015). Semen samples were collected from male rhesus macaques and sperm was prepared as previously described (Wolf et al., 1989). Collected sperm and/or oocytes were treated with S3 prior to IVF for 3 to 7 hours in the following combinations: 1) vehicle (100% DMSO) treated oocytes + vehicle treated sperm, 2) vehicle treated oocytes + S3 treated sperm, 3) S3 treated oocytes + vehicle treated sperm, and 4) S3 treated oocytes + S3 treated sperm. Two sets of experiments were performed, with S3 at a final concentration of 2 μM (n = 3 animals) and 20 μM final concentration (n = 3 animals). Cumulus-oocyte complexes were collected and IVF was performed using freshly collected sperm. Sperm and cumulus-oocyte complexes were co-cultured in 100 μl droplets covered with oil for 18 – 24 hours, at which point they were then transferred into dishes (Life Global LLC, Guilford, CT) containing fresh Global Medium (Global Cell Solutions, North Garden, VA). Fertilization was determined 24 hours later by visualization that the first cleavage stage was completed.

2.8 OPC culture maturation analysis

Mouse (C57BL/6) OPCs generated from neural stem cells were plated on poly-L-ornithine–coated coverslips in OPC medium. After 24 hours, the medium was switched to differentiation medium comprised of DMEM/F12, 0.1% BSA, 2% B27 supplement, 30 nM T3 and 5 μg/ml NAC (Sigma). Cells were treated with vehicle, HMW HA (50 μg/ml), HMW HA and 1 μM S3, HA and 1 μM S3 with rbPH20 (250 ng/ml) or Vcpal (25 μM) for 96 hours. Cells were fixed in 4% paraformaldehyde and analyzed for OPC maturation by immunohistochemistry.

For cell counts, 20 fields were randomly selected, and in each field at least 500 cells were counted as either PDGFRα- or MBP-positive per coverslip (4 coverslips per group). The experiment was performed a total of 3 times. Mean cell numbers and standard deviations were calculated for each group.

2.9 Forebrain slice culture

Whole forebrain coronal slices (300 μm; collected at the level of the mid-rostral corpus callosum and anterior septal nuclei; 3 adjacent slices from each brain) were collected from P0/1 rat pups for organotypic cultures prepared as previously described (Dean et al., 2011). Only the forebrain slices with a complete corpus callosum were used for cultures. Briefly, brains were embedded in 4% low melting point agar (Invitrogen) and sectioned into sterile ice-cold complete Hank's balanced salt solution (HBSS, Ca^{2+}/Mg^{2+} free; Invitrogen), supplemented with 30 mM D-glucose, 2.5 mM HEPES buffer, 1 mM $CaCl_2$, 1 mM $MgSO_4$, 4 mM $NaHCO_3$, and 0.001% phenol red (Sigma) using a VTS 1600 vibrating microtome (Leica Microsystems Inc.). Isolated slices were transferred onto 0.4 μm porous membrane cell culture inserts (Becton Dickinson) that were pre-coated with laminin/poly-D-lysine (Sigma), and cultured in slice culture media (Basal Medium Eagle (Invitrogen), supplemented with complete HBSS [25% v/v], 27 mM D-glucose, 100 U/ml penicillin and streptomycin, 1 mM glutamine and 5% horse serum (New Zealand origin, heat inactivated; Invitrogen). Slices were incubated at 37 °C/5% CO_2, and the growth medium changed every other day. Slices were cultured for 7–8 days.

Cell counts in slice cultures were performed using a Stereo-Investigator stereology system (MBP Bioscience). Cell counts were made within the boundaries of the corpus callosum observed at low power (10x) defined by DAPI-staining. Estimates of MBP-labeled cells in the entire corpus callosum were obtained using the meander scan function at 20x.

2.10 Analysis of AKT phosphorylation

Equivalent amounts of total protein from cell lysates were analyzed by SDS-PAGE and transferred to an Immobilon-FL membrane, then probed with either a mouse monoclonal anti-actin antibody (1:4,000; 8H10D10) or an anti-phospho-AKT S473 antibody (1:1,000; 9271), both from Cell Signaling Technology, Inc. as previously described (Srivastava et al., 2018). Pixel band intensities were analyzed with the Odyssey Infrared system (Li-COR Biosciences).

2.11 Lysolecithin Lesions

Demyelination was induced in the rostral corpus callosum of 3–4 month old C57BL/6J mice by injection of lysolecithin (2% in PBS; Sigma) at 5.5 mm anterior to lambda and 1 mm lateral to bregma, and 2.5 mm deep as previously described (Back et al., 2005) mixed with either vehicle (PBS) or different concentrations of S3. Brains were harvested at 8-days post-lysolecithin injection and processed for compound action potential recordings and then fixed for immunohistochemistry as outlined below and as previously described (Preston et al., 2013).

2.12 Compound action potential (CAP) recordings

Brains were rapidly removed and submerged in ice cold artificial cerebrospinal fluid (aCSF; 124 mM NaCl, 5 mM KCl, 1.25 mM NaH_2PO_4, 26 mM $NaHCO_3$, 1.3 mM $MgSO_4$, 2 mM $CaCl_2$, 10 mM glucose, pH 7.4) saturated with 95% O_2/5% CO_2. Four hundred micrometer thick coronal slices corresponding to Bregma coordinates 0.5 to 0.9 were cut on a vibratome (Leica), collected, and incubated in aerated aCSF at room temperature for 1 hour prior to recordings. For recordings, the slice was transferred to a perfusion chamber mounted on an upright microscope (Zeiss). The tract of the injection electrode was usually visible, however, injection sites were confirmed with subsequent histochemical analysis of the slice. Recording and stimulating electrodes were positioned in the corpus callosum on the side of the injection and then moved to the opposite side to obtain recordings of untreated axons. The bipolar stimulating electrodes were fashioned from teflon-insulated tungsten wires (WPI) with tips positioned approximately 0.3 mm apart. The stimulating electrodes were connected to a stimulator (Grass S88) and stimulation isolation unit (Grass). Stimulus intensity was adjusted to obtain a maximal response. Recordings were obtained using glass microelectrodes filled with aCSF with a resistance of 3–5 Megaohm. Recordings were amplified and filtered at 10 kHz. Recordings were obtained from 2 sites across the width of the corpus callosum at approximately 1.5 mm from the stimulating electrode. Ten responses were averaged at each recording site. The stimulus was 50–200 microsec. duration; 0.5–5 mA (to evoke max response). Stimulus artifact was trimmed from the trace at the origin of the trace. The magnitude of the CAP waveform was determined by measuring the maximum negative deflection with respect to a tangent drawn between the adjacent positive deflections. For each recording session 3 animals per group (treated with S3 or vehicle) were analyzed.

2.13 Immunohistochemistry

Following long-term slice cultures or CAP recordings, tissue slices were immersion fixed for 12–16 hrs in 4% paraformaldehyde at 4°C, rinsed three times in PBS at room temperature, then cyroprotected in 30% sucrose overnight at 4°C. Tissues were embedded in Optimal Cutting Temperature medium, rapidly frozen on dry ice and cryosectioned at a thickness of 25 μm. Cells and tissues were pre-blocked in 10% heat-inactivated fetal bovine serum for 45 minutes. Primary antibodies were diluted in blocking buffer and tissues were incubated overnight at 4°C, rinsed in blocking buffer three times, then incubated with the appropriate species-specific fluoro-conjugated secondary antibodies (Alexa546 or Alexa488, Molecular Probes Inc.) overnight. Antibodies used were: rat anti-PDGF receptor-alpha (PDGFRα; 1:250, BD Pharminagen), mouse anti-O4 (1:500, Millipore), mouse anti-myelin basic protein (MBP; 1:1000, Sternberger Monoclonal), rabbit anti-O1 (1:100, Millipore), rabbit anti-neurofilament light chain (NF-L; 1:1000, Millipore), and mouse anti-CC1 (1:200, Calbiochem). Biotinylated HA-binding protein (bHABP; 1:250, Calbiochem) was used in place of a primary antibody and Cy3-streptavidin (1:2000, Jackson Lba) in place of a secondary antibody to visualize HA.

Cells and tissues were imaged by fluorescence microscopy using either a Zeiss Axioskop 40 epifluorescent upright microscope or a Leica SP5 AOBS confocal system. Confocal images were acquired using a 40x NA 1.25 Pl-Apo objective (zoom 4, pinhole 1 Airy unit). For

double immunofluorescent staining, data from two channels were collected by sequential scanning. Z-stacks of images were collected to generate Z projections.

2.14 Statistical Analysis

Statistical analysis of fertilization rates was performed using logistic regression analysis to determine significance between treatments groups in each of the dose groups. An unpaired two-tailed t-test was used to compare changes in anti-PDGF-Rα and anti-MBP immunolabeled cells in *in vitro* experiments. One-way analysis of variance (ANOVA) followed by Tukey's multiple comparison test was used to assess changes in the percentages, relative to controls, of mature OL's in cultures treated with Vcpal. A value of $p < 0.05$ was considered significant.

3. RESULTS

3.1 Specific modified forms of apigenin are potent hyaluronidase inhibitors

To assess if modified flavonoids with an apigenin-based structure can function as effective inhibitors of extracellular hyaluronidases with activities at neutral pH, we synthesized six distinct apigenin-based modified flavonoids as previously described (Srinivasa et al., 2014; see also Fig. 1A) then tested their ability to inhibit HMW HA digestion by bovine testicular hyaluronidase (BTH) at pH 7.0 after 1 hour at 37 °C. The preparations of HMW HA include a wide range of molecular weights and appear as a range of sizes in agarose gels whose overall MW shifts with HA digestion. Using image analysis, we marked the highest size in each lane with a black bar (Fig. 1B). All of the agents at least partially inhibited HA digestion at 200 μM (Fig. 1B) with nearly complete inhibition by three agents (S1, S3, and S6). At 20 μM, S3 demonstrated the greatest inhibition of HA digestion (Fig 1C), and showed significant inhibition at concentrations as low as 2 μM (Fig. 1D). We determined the structure of S3 to be [(2-Chloroacetyl)(P-chloro)amino]-2-(7-hydroxy-4-oxo-3-chromenyl)-1-(tert-butylamino)-1-ethanone based on NMR and mass spectroscopy (data not shown). Each of these compounds was more effective at blocking HA digestion by BTH than Vcpal and by the previously described indole carboxamide inhibitors N-(4-fluorobenzyl)-1-benzyl-1H-indole-2-carboxamide and N-(4-chlorobenzyl)-1-(4-fluorobenzyl)-1H-indole-3-carboxamide (Kaessler et al., 2011 and data not shown).

3.2 The S3 modified flavonoid is a selective hyaluronidase inhibitor

Because the S3 agent was the most effective BTH inhibitor, we chose to further characterize the effects of S3 on the activities of other hyaluronidases. Previously described hyaluronidase inhibitors inhibit multiple mammalian hyaluronidases. We therefore compared the ability of S3 to inhibit recombinant PH20 (rPH20, which constitutes the major hyaluronidase activity in BTH), recombinant Hyal1, and *Streptomyces* hyaluronidase. We determined the optimal concentration of each enzyme that maximally digested HMW HA at either pH 7.0 (rPH20 and *Streptomyces* hyaluronidase) or pH 4.0 (Hyal1) after 1 hr. at 37 °C. We attempted to test a recombinant preparation of Hyal2 as well, but we could not detect hyaluronidase activity under any conditions (data not shown). We found that S3 effectively blocked rPH20 and *Streptomyces* hyaluronidase, but not Hyal1 (Fig 2A, D).

As a second approach to test the specificity of S3 for specific hyaluronidases, we transfected HEK-293T cells with expression vectors carrying cDNAs for either *PH20*, *Hyal1*, *Hyal2*, or cDNAs encoding transmembrane protein 2 (*TMEM2*) or the cell migration-inducing and HA-binding protein (*CEMIP*), then generated cell lysates mixed with HMW HA. Lysates from cells transfected with *PH20*, *Hyal1*, *Hyal2* digested HMW HA (Fig. 2B) while lysates from cells transfected with vector alone demonstrated no hyaluronidase activity (Fig. 2C). TMEM2 has been reported to act as a cell surface hyaluronidase in 293T cells (Yamamoto et al., 2017). However, we were unable to observe any HA-depolymerizing activity in cells transfected with *TMEM2* (data not shown) in agreement with findings reported in skin cells (Yoshino et al., 2018). However, consistent with previous findings (Yoshida et al., 2013) live cultures of HEK293T cells expressing CEMIP digested HMW HA that was added to the cultures (Fig. 2C). The effects of cultures expressing PH20 or CEMIP on HMW HA digestion were inhibited by S3 (Fig. 2B, 2C, 2D). The effects of S3 on CEMIP activity are interesting in light of a report suggesting that CEMIP is elevated in demyelinating lesions from patients with MS (Marella et al., 2018). However, S3 had no effect on HA digestion by lysates (not shown) or live cultures (Fig. 2D) of cells transfected with Hyal1 or Hyal2 expression vectors. All together, these data indicate that S3 is a more selective inhibitor of hyaluronidase activity than Vcpal.

In addition to inhibiting hyaluronidases, apigenin is a potent inhibitor of matrix metalloproteinase activity (Kuppusamy et al., 1990; Hertel et al., 2006; Sim et al., 2007). Srinivasa and co-workers (2014) previously demonstrated that modified apigenin-based flavonoids could similarly inhibit metalloproteinase activity in the venom of *Echis carinatus*, the saw-scaled viper. To determine if S3 similarly inhibits metalloproteinase activity, we performed zymography assays testing if S3 can inhibit gelatinolytic, caseinolytic, fibrinolytic and fibronogenolytic activity when mixed with 2 μg of *Echis carinatus* venom. As shown in Fig. 3, S3 effectively blocked gelatinolytic (Fig. 3A) and caseinolytic (Fig. 3B) activity at concentrations ≥100 μM and fibrinogenolytic activity at concentrations ≥500 μM (Fig. 3C). Fibrinolytic activity was partially blocked (with some protection of the α-chain) at S3 concentrations ≥10 μM, with full inhibition at concentrations ≥500 μM (Fig. 3D). Given that we observed inhibition of hyaluronidase activity at ≤2 μM (Fig. 1D), these data indicate that S3 has a high degree of specificity to block hyaluronidases but not multiple classes of metalloproteinases at low micromolar concentrations.

3.3 The S3 inhibitor can block fertilization

PH20 is expressed by mammalian sperm and facilitates sperm entry into eggs possibly by digesting extracellular HMW HA secreted by the cumulus cells surrounding the oocyte and/or through promoting sperm binding to the zona pellucida, a glycoprotein layer encasing mammalian oocytes (Hunnicutt et al., 1996; Yudin et al., 1999). Function-blocking antibodies against PH20 block pig oocyte fertilization in *in vitro* fertilization assays (Yoon et al., 2014). We therefore tested if S3 could block fertilization. We performed *in vitro* fertilization in which oocytes and/or sperm from rhesus macaques were treated with vehicle or either 2 μM or 20 μM S3. As shown in Table 1, treatment of either sperm, oocytes, or both with 2 μM S3 resulted in up to a 30% reduction in fertilization, while treatment with 20 μM S3 resulted in a nearly complete inhibition of fertilization. The difference between overall

dosage effects was highly significant ($p<0.0001$). We observed no changes in either sperm or oocyte viability following S3 treatment (data not shown). These findings are consistent with the notion that S3 can inhibit extracellular hyaluronidase activity.

3.4 Selective inhibition of hyaluronidase activity promotes OPC maturation *in vitro*

As discussed above, Vcpal is a broad spectrum inhibitor of hyaluronidases that blocked HA degradation in cultures of OPCs and increased the proportion of cells that became mature OLs (Botzki et al., 2004; Sloane et al., 2010; Preston et al., 2013). However, Vcpal also can function as an anti-oxidant and inhibits other enzymes including lipoxygenases. Given the greater selectivity of S3 for hyaluronidases with activities that are similar to that of PH20, we determined if S3 can reverse the inhibitory effects of added HMW HA on OPC maturation *in vitro*. While HMW HA significantly inhibited OPC maturation (compare Fig. 4A and 4B; and see Fig. 4F) as previously described (Back et al., 2005; Sloane et al., 2010), treatment with S3 overcame the effects of HMW HA (Fig. 4C, F). Interestingly, S3 at 2 μM was more effective at promoting OPC maturation than Vcpal at 25 μM (compare Fig. 4C and 4E; and see Fig. 4F). We did not observe any changes in OPC maturation if S3 was added to cultures in the absence of HMW HA (Fig. 4F). We also did not observe any significant changes in total cell numbers or on cell death in cultures treated with these concentrations of S3 (data not shown), indicating that S3 was directly impacting OPC maturation.

To demonstrate that the effects of S3 on OPC maturation were dependent on blocking hyaluronidase activity, we treated cultures with increasing amounts of rPH20. We reasoned that this approach would demonstrate specificity because: (1) We have clearly shown that S3 blocks rPH20 activity; (2) the digestion products generated by PH20 are sufficient to block OPC maturation and remyelination (e.g. Preston et al., 2013; Srivastava et al., 2018); (3) No activities other than HA depolymerization have been attributed to PH20, which has been carefully studied both in basic and commercial settings, and has been examined for off target effects in clinical trials (e.g. Infante et al., 2018); and (4) The effects of HMW HA on OPC maturation can be blocked in OPC cultures and in *in vivo* models of demyelination by Vcpal (e.g. Sloane et al., 2010; Preston et al., 2013; 73:266-80; Srivastava et al., 2018). We found that the effects of S3 were reversed if cultures were treated with 25 U of recombinant PH20 (Fig. 4D, F). Thus, both Vcpal, a non-specific hyaluronidase inhibitor, and S3 overcome the effects of HMW HA on OPC maturation, consistent with the hypothesis that the hyaluronidase activity exhibited by OPCs impairs OPC maturation.

3.5 Blocking hyaluronidase activity promotes OPC maturation in an *in vitro* model of white matter injury

Previous studies suggested that digestion products generated by hyaluronidase activity in demyelinating lesions contribute to myelination delay or remyelination failure following insults to the CNS (Sloane et al., 2010; Preston et al., 2013; Hagen et al., 2014). To investigate whether hyaluronidase activity from OPCs attenuates OL maturation following perinatal CNS injury, we employed an *in vitro* slice culture model of perinatal white matter injury (Dean et al., 2011). In this model, extensive reactive astrogliosis is accompanied by high levels of hyaluronidase activity such that adding HMW HA to cultures generates bioactive HA digestion products that inhibit OPC maturation (Srivastava et al., 2018). As

shown in Fig. 5A, a composite image of one such slice, the majority of MBP+, olig2+ cells continue to reside in the white matter (outlined area) in these slices throughout the culture period, with some superficial MBP+ cells scattered throughout the cortex. We identified the white matter/cortex boundaries using DAPI staining and olig2 immunolabeling (e.g. outlined area in Fig. 5A). We then used these boundaries to draw white matter regions of interest. Then, under higher magnification, the cells that were immunoreactive for specific markers were counted. We found that treatment of the slices with BTH further inhibited OL maturation as indicated by significant reductions in MBP expression throughout the white matter (Fig. 5B–F) and reduced numbers of O1+ but not O4+ cells (Fig. 5G–I). These effects are reflected by an overall reduction in mature OLs (Fig. 5I). We saw a similar degree of inhibition when using recombinant PH20 in place of BTH (Fig. 5J) ruling out the possibility that the effects we observed with BTH were due to growth factor contamination as suggested in an earlier study (Marella et al., 2017).

We next assessed whether blocking endogenous hyaluronidase activity could promote OPC maturation in the slice cultures. In these experiments, mature OLs were identified and counted based on their morphology and MBP immunoreactivity (Fig. 6A–C). Slices were treated with vehicle alone (Fig. 6D), HMW HA and vehicle (Fig. 6E), or HMW HA and S3 (2 μM) (Fig. 6F). Cultures treated with HMW HA demonstrated significant reductions in MBP immunostaining compared to cultures treated with vehicle alone (Fig. 6D, E; 6G). In contrast, cultures treated with S3 in the presence of HMW HA demonstrated accelerated OL maturation (Fig. 6F, G). We observed no significant changes in MBP immunostaining in cultures treated with S3 alone (Fig. 6G). These data indicate that it is de-polymerization of HMW HA within the injury microenvironment that ultimately regulates OL maturation in the setting of white matter injury.

3.6 Blocking hyaluronidase activity reverses signaling linked to maturation arrest in OPCs

Elevated AKT phosphorylation is linked to enhanced CNS myelination (Flores et al., 2008). We previously found that bioactive HA digestion products signal through a toll-like receptor-4-dependent pathway to reduce AKT phosphorylation and block OPC maturation (Srivastava et al., 2018). Therefore, if S3 promotes OPC maturation by blocking hyaluronidase activity, S3 treatment should reverse reduced AKT phosphorylation induced by HMW HA. Consistent with previous findings (Srivastava et al., 2018), we find that at both 3 and 5 days in culture, HMW HA induces reduced AKT phosphorylation at serine 473 compared to vehicle-treated controls (Fig. 7A, B). At both time points, S3 increased serine 473 phosphorylation to levels above vehicle-treated cultures, consistent with signaling that enhances remyelination (Fig. 7A, B).

3.7 Selective inhibition of hyaluronidase activity accelerates functional remyelination

We previously reported that Vcpal promoted functional remyelination in lysolecithin-induced demyelinated lesions with added HMW HA in the mouse corpus callosum (Preston et al., 2013). We therefore tested if S3 could similarly promote functional remyelination in lysolecithin lesions. Surprisingly, we found that intracranial injections of S3 into the corpus callosum following lysolecithin treatment without added HMW HA resulted in a

significant increase (approximately 60% of uninjected controls) in conduction velocities through lysolecithin-induced lesions compared to animals treated with vehicle (Fig. 8A–D). When the slices used for recordings were immunostained for MBP and neurofilament, S3-treated animals consistently demonstrated elevated MBP immunoreactivity within lesion borders by 8 days post-injection, while vehicle controls remained demyelinated (Fig. 8E–J). Interestingly, we found that HA is elevated both at lesion borders and to a lesser extent within these lesions (Fig. 8E, inset), indicating that HA is elevated in lysolecithin lesions. When we examined MBP and neurofilament staining within lesions using laser confocal microscopy at higher magnification, we found that lesions treated with S3 demonstrated MBP immunoreactivity associated with neurofilament-labeled axons while control lesions demonstrated little if any myelin associated with axons (Fig. 8I, J). All together, these data indicate that blocking specific forms of hyaluronidase activity within demyelinating lesions can promote functional remyelination.

4. DISCUSSION

We and others previously reported that digestion products of HMW HA could block OPC maturation and that OPCs express a variety of hyaluronidases (Sloane et al., 2010; Preston et al., 2013). Furthermore, we previously found that overexpression of two hyaluronidases that digest extracelluar HMW HA at neutral pH, PH20 and HYAL5, both inhibited OPC maturation, and that partial digestion products of PH20 but not another hyaluronidase inhibited remyelination (Preston et al., 2013). We further found that Vcpal, which has a number of biological activities including inhibition of multiple hyaluronidases, could promote functional remyelination (Preston et al., 2013). These findings suggested that specific hyaluronidases expressed by OPCs generate HA digestion products that block OPC maturation and remyelination, and that agents that inhibit specific hyaluronidases could be used to promote remyelination in demyelinating conditions. Here, we characterized a novel hyaluronidase inhibitor, S3, that inhibits PH20, CEMIP and *Streptomyces* hyaluronidase activity but not Hyal1 or Hyal2. At concentrations that inhibit hyaluronidase but not metalloproteinase activity, we found that S3 reverses the effects of HMW HA AKT phosphorylation and OPC maturation in OPCs grown *in vitro.* The finding that S3 overcame HMW HA-mediated inhibition of OPC maturation in conjunction with the finding that the effects of S3 could be overcome by adding PH20 to OPC cultures confirm that S3 was acting by inhibiting hyaluronidase activity in these cultures. We further find that S3 promotes OPC maturation in an *in vitro* model of perinatal white matter injury and functional remyelination in an *in vivo* model of adult demyelination. These findings indicate that: (1) hyaluronidase activity within demyelinating lesions is sufficient to block OPC maturation and remyelination; (2) hyaluronidase activity from OPCs can generate sufficient HA digestion products to block their own maturation; and (3) that modified flavonoids which target hyaluronidase activity could be efficacious in treating conditions where myelination is delayed or where remyelination fails.

Multiple mechanisms have been implicated in preventing OPC maturation following CNS injuries. For example, activation of the canonical Wnt signaling cascade leads to a delay in OPC differentiation (Fancy et al., 2009; Feigenson et al., 2009; Guo et al., 2015). Signals that block activation of AKT have also been implicated in regulating

developmental myelination and remyelination (reviewed by Gaesser and Fyffe-Maricich, 2016), while the Leucine rich repeat and Immunoglobulin-like domain-containing Nogo receptor interacting protein 1 (LINGO-1) acts as a negative regulator of OPC differentiation through a mechanism that includes downregulation of gelsolin, an abundant actin-severing protein involved in the depolymerization of actin filaments (Mi et al., 2005; Mi et al., 2013; Shao et al., 2017). In contrast, estrogen receptor-β agonists have been implicated in promoting functional remyelination (reviewed by Khalaj et al., 2017). Interestingly, HA and its receptor, CD44, can influence each of these pathways. CD44, for example, can regulate Wnt-induced β-catenin signaling (Chang et al., 2013; Schmitt et al., 2015); CD44-HA interactions can influence AKT activity which may in turn induce further HA synthesis (e.g. Liu and Cheng, 2017; Zhu et al., 2013); similar to the effects of LINGO-1, low molecular weight forms of HA lead to reduced levels of gelsolin (Lee et al., 2014); and estradiol can influence HA synthesis (Freudenberger et al., 2011). Thus, signaling by HA through CD44 or other HA receptors (e.g. Toll-Like receptors; Termeer et al., 2002; Jiang et al., 2005; Scheibner et al., 2006; Taylor et al., 2007; Garantziotis et al., 2010; Li et al., 2011; Campo et al., 2012; Foley et al., 2012; Sloane et al., 2010; Black et al., 2013; Riehl et al., 2015; Sunabori et al., 2016; Liang et al., 2016; Srivastava et al., 2018) may affect multiple signaling pathways in OPCs that regulate OPC maturation. How different sizes of HA digestion products induce distinct signaling is unclear. Different HA digestion products may influence receptor-HA conformational changes that enable transmembrane-mediated activation of cytoplasmic domains or specific HA sizes may enable multiple receptors to bind the same HA, creating different cytoplasmic signaling complexes that together influence OPC maturation (Weigel and Baggenstoss, 2017).

The specific hyaluronidase or hyaluronidases which generate HA digestion products that block OPC maturation are unknown. We and others reported that the PH20 hyaluronidase is transiently expressed following a variety of insults to the CNS (Sloane et al., 2010; Preston et al., 2013; Hagen et al., 2014; Xing et al., 2014; Sherman and Back, 2017). However, in our experience PH20 transcripts are only expressed transiently and at very low abundance in injured CNS tissues (unpublished findings). Furthermore, one study failed to find PH20 expression in either the normal or injured CNS (Marella et al., 2017). It is possible therefore that other extracellular HA-depolymerizing enzymes that function at neutral pH could generate HA digestion products that block OPC maturation. Likely candidates include TMEM-2, which is expressed by OLs (Golan et al., 2008; Marques et al., 2016) and CEMIP, which is expressed in the CNS and which is elevated in both rodent and human demyelinating lesions (Yoshino et al., 2017; Marella et al., 2018).

The S3 hyaluronidase inhibitor characterized here is a modified form of the flavonoid apigenin. Flavonoids are polyphenols found in a variety of plants including vegetables and fruits. All flavonoids share a 15-carbon structure that includes two benzene rings that are linked by a heterocyclic pyrane ring. Multiple natural flavonoids can inhibit hyaluronidase activity to varying degrees (e.g. Rodney et al. 1950; Kuppusamy et al., 1990; Li et al., 1997; Hertel et al., 2006; Zeng et al., 2015) by binding directly into the enzyme cavity site, which influences the enzyme microenvironment and reduces activity (Zeng et al., 2015). We demonstrate here that this inhibitory activity can be enhanced by relatively modest chemical modifications to flavonoid structures. We also found that these modifications can alter the

specificity of flavonoids for different enzymes and even for different hyaluronidases, making these compounds excellent candidates for therapeutic applications. In addition, multiple flavonoids or their metabolites can cross the blood-brain-barrier (e.g. Krasieva et al., 2015; Wang et al., 2012; Schaffer and Halliwell, 2012; Vauzour, 2012), reaching concentrations between 40 pmol and 0.5 nmol/g of tissue (Schaffer and Halliwell, 2012; Vauzour, 2012). These data suggest that low micromolar concentrations of flavonoids *in vitro*, such as those used in this study, should reflect reasonable physiological levels for inhibiting hyaluronidase activity and promoting remyelination *in vivo* following systemic administration.

Although we are the first to demonstrate that flavonoids can directly promote OPC maturation and remyelination, several flavonoids are reported to have neuroprotective activity as well as neuroimmunomodulatory activity (reviewed by Jaeger et al., 2017; Spagnuolo et al., 2017). Apigenin and hesperidin, for example, can both reduce neuroinflammation in rodents with experimental autoimmune encephalomyelitis, a model of multiple sclerosis (Ginwala et al., 2016; Ciftci et al., 2015; Haghmorad et al., 2017). Quercetin has neuroprotective activities following hypoxia (Pandey et al., 2012). Scutellarin, another flavonoid, reduces the severity of cuprizone-induced demyelination, possibly by preventing neural stem cell apoptosis and subsequent oligodendrocyte differentiation (Wang et al., 2016). This finding is interesting in light of our recent report demonstrating that HA regulates neural stem cell proliferation and neurogenesis in the hippocampal dentate gyrus (Su et al., 2017). All together, these studies and the data presented here suggest that flavonoids have a wide range of potential therapeutic applications in the CNS, and that these activities can be enhanced through simple chemical modifications.

ACKNOWLEDGEMENTS

We thank Byung Park of the Oregon National Primate Research Center (ONPRC) Biostatistics and Bioinformatics Unit for the statistical analysis, the ONPRC Assisted Reproductive Technologies Support Core, and the ONPRC Integrated Pathology Core Imaging Services for their assistance in providing the materials and equipment needed to complete these experiments. This work was supported by P51 OD011092 for the operation of the Oregon National Primate Research Center, MS160144 from the Congressionally Directed Medical Research Programs and RG 4843A5/1 and PP-1801-29683 from the National Multiple Sclerosis Society (to LSS) and NS054044 and NS045737 from the National Institute of Neurological Disorders and Stroke and American Heart Grant in Aid #17GRNT33370058 (to SAB).

REFERENCES

Back SA, Tuohy TM, Chen H, Wallingford N, Craig A, Struve J, Luo NL, Banine F, Liu Y, Chang A, Trapp BD, Bebo BF Jr, Rao MS, & Sherman LS (2005). Hyaluronan accumulates in demyelinated lesions and inhibits oligodendrocyte progenitor maturation. Nat Med. 11, 966–72. doi: 10.1038/nm1279 [PubMed: 16086023]

Black KE, Collins SL, Hagan RS, Hamblin MJ, Chan-Li Y, Hallowell RW, Powell JD, & Horton MR (2013). Hyaluronan fragments induce IFNβ via a novel TLR4-TRIF-TBK1-IRF3-dependent pathway. J Inflamm (Lond). 10, 23. doi: 10.1186/1476-9255-10-23 [PubMed: 23721397]

Botzki A, Rigden DJ, Braun S, Nukui M, Salmen S, Hoechstetter J, Bernhardt G, Dove S, Jedrzejas MJ, & Buschauer A (2004). L-Ascorbic acid 6-hexadecanoate, a potent hyaluronidase inhibitor. X-ray structure and molecular modeling of enzyme-inhibitor complexes. J Biol Chem. 279, 45990–7. doi: 10.1074/jbc.M406146200 [PubMed: 15322107]

Bugiani M, Postma N, Polder E, Dieleman N, Scheffer PG, Sim FJ, van der Knaap MS, & Boor I (2013). Hyaluronan accumulation and arrested oligodendrocyte progenitor maturation in vanishing white matter disease. Brain 136, 209–22. doi: 10.1093/brain/aws320 [PubMed: 23365098]

Buser JR, Maire J, Riddle A, Gong X, Nguyen T, Nelson K, Luo NL, Ren J, Struve J, Sherman LS, Miller SP, Chau V, Hendson G, Ballabh P, Grafe MR, & Back SA (2012). Arrested preoligodendrocyte maturation contributes to myelination failure in premature infants. Ann Neurol. 71, 93–109. doi: 10.1002/ana.22627 [PubMed: 22275256]

Campo GM, Avenoso A, D'Ascola A, Prestipino V, Scuruchi M, Nastasi G, Calatroni A, & Campo S (2012). Hyaluronan differently modulates TLR-4 and the inflammatory response in mouse chondrocytes. Biofactors 38, 69–76. doi: 10.1002/biof.202 [PubMed: 22287316]

Cargill R, Kohama SG, Struve J, Su W, Banine F, Witkowski E, Back SA, & Sherman LS (2012). Astrocytes in aged nonhuman primate brain gray matter synthesize excess hyaluronan. Neurobiol Aging 33, 830.e13–24. doi: 10.1016/j.neurobiolaging.2011.07.006

Chang G, Zhang H, Wang J, Zhang Y, Xu H, Wang C, Zhang H, Ma L, Li Q, & Pang T (2013). CD44 targets Wnt/β-catenin pathway to mediate the proliferation of K562 cells. Cancer Cell Int. 13, 117. doi: 10.1186/1475-2867-13-117 [PubMed: 24257075]

Chowdhury B, Hemming R, Faiyaz S, & Triggs-Raine B (2016). Hyaluronidase 2 (HYAL2) is expressed in endothelial cells, as well as some specialized epithelial cells, and is required for normal hyaluronan catabolism. Histochem Cell Biol. 145, 53–66. doi: 10.1007/s00418-015-1373-8 [PubMed: 26515055]

Ciftci O, Ozcan C, Kamisli O, Cetin A, Basak N, & Aytac B (2015). Hesperidin, a Citrus Flavonoid, Has the Ameliorative Effects Against Experimental Autoimmune Encephalomyelitis (EAE) in a C57BL/J6 Mouse Model. Neurochem Res. 40, 1111–20. doi: 10.1007/s11064-015-1571-8 [PubMed: 25859982]

Cole KLH, Early JJ, & Lyons DA (2017). Drug discovery for remyelination and treatment of MS. Glia 65, 1565–1589. doi: 10.1002/glia.23166. [PubMed: 28618073]

Csóka AB, Frost GI, Heng HH, Scherer SW, Mohapatra G, & Stern R (1998). The hyaluronidase gene HYAL1 maps to chromosome 3p21.2-p21.3 in human and 9F1-F2 in mouse, a conserved candidate tumor suppressor locus. Genomics 48, 63–70. [PubMed: 9503017]

Dean JM, Riddle A, Maire J, Hansen KD, Preston M, Barnes AP, Sherman LS, & Back SA (2011). An organotypic slice culture model of chronic white matter injury with maturation arrest of oligodendrocyte progenitors. Mol Neurodegener. 6, 46. doi: 10.1186/1750-1326-6-46 [PubMed: 21729326]

De Angelis JE, Lagendijk AK, Chen H, Tromp A, Bower NI, Tunny KA, Brooks AJ, Bakkers J, Francois M, Yap AS, Simons C, Wicking C, Hogan BM, & Smith KA (2017). Tmem2 Regulates Embryonic Vegf Signaling by Controlling Hyaluronic Acid Turnover. Dev Cell 40, 123–136. doi: 10.1016/j.devcel.2016.12.017 [PubMed: 28118600]

Fancy SP, Baranzini SE, Zhao C, Yuk DI, Irvine KA, Kaing S, Sanai N, Franklin RJ, & Rowitch DH (2009). Dysregulation of the Wnt pathway inhibits timely myelination and remyelination in the mammalian CNS. Genes Dev. 23, 1571–85. doi: 10.1101/gad.1806309 [PubMed: 19515974]

Feigenson K, Reid M, See J, Crenshaw EB 3rd, & Grinspan JB (2009). Wnt signaling is sufficient to perturb oligodendrocyte maturation. Mol Cell Neurosci. 42, 255–65. doi: 10.1016/j.mcn.2009.07.010 [PubMed: 19619658]

Foley JP, Lam D, Jiang H, Liao J, Cheong N, McDevitt TM, Zaman A, Wright JR, & Savani RC (2012). Toll-like receptor 2 (TLR2), transforming growth factor-β, hyaluronan (HA), and receptor for HA-mediated motility (RHAMM) are required for surfactant protein A-stimulated macrophage chemotaxis. J Biol Chem. 287, 37406–19. doi: 10.1074/jbc.M112.360982 [PubMed: 22948158]

Franklin RJM & Ffrench-Constant C (2017). Regenerating CNS myelin - from mechanisms to experimental medicines. Nat Rev Neurosci. 18, 753–769. doi: 10.1038/nrn.2017.136 [PubMed: 29142295]

Freudenberger T, Röck K, Dai G, Dorn S, Mayer P, Heim HK, & Fischer JW (2011). Estradiol inhibits hyaluronic acid synthase 1 expression in human vascular smooth muscle cells. Basic Res Cardiol. 106,1099–109. doi: 10.1007/s00395-011-0217-5 [PubMed: 21901291]

Gaesser JM & Fyffe-Maricich SL (2016). Intracellular signaling pathway regulation of myelination and remyelination in the CNS. Exp Neurol. 283, 501–11. doi: 10.1016/j.expneurol.2016.03.008 [PubMed: 26957369]

Ginwala R, McTish E, Raman C, Singh N, Nagarkatti M, Nagarkatti P, Sagar D, Jain P, & Khan ZK (2016). Apigenin, a Natural Flavonoid, Attenuates EAE Severity Through the Modulation of Dendritic Cell and Other Immune Cell Functions. J Neuroimmune Pharmacol. 11,36–47. doi: 10.1007/s11481-015-9617-x [PubMed: 26040501]

Garantziotis S, Li Z, Potts EN, Lindsey JY, Stober VP, Polosukhin VV, Blackwell TS, Schwartz DA, Foster WM, & Hollingsworth JW (2010). TLR4 is necessary for hyaluronan-mediated airway hyperresponsiveness after ozone inhalation. Am J Respir Crit Care Med. 181,666–75. doi: 10.1164/rccm.200903-0381OC [PubMed: 20007931]

Golan N, Adamsky K, Kartvelishvily E, Brockschnieder D, Möbius W, Spiegel I, Roth AD, Thomson CE, Rechavi G, & Peles E (2008). Identification of Tmem10/Opalin as an oligodendrocyte enriched gene using expression profiling combined with genetic cell ablation. Glia 56,1176–86. doi: 10.1002/glia.20688 [PubMed: 18571792]

Guo F, Lang J, Sohn J, Hammond E, Chang M, & Pleasure D (2015). Canonical Wnt signaling in the oligodendroglial lineage--puzzles remain. Glia 63, 1671–93. doi: 10.1002/glia.22813. [PubMed: 25782433]

Hagen MW, Riddle A, McClendon E, Gong X, Shaver D, Srivastava T, Dean JM, Bai JZ, Fowke TM, Gunn AJ, Jones DF, Sherman LS, Grafe MR, Hohimer AR, & Back SA (2014). Role of recurrent hypoxia-ischemia in preterm white matter injury severity. PLoS One 9, e112800. doi: 10.1371/journal.pone.0112800 [PubMed: 25390897]

Haghmorad D, Mahmoudi MB, Salehipour Z, Jalayer Z, Momtazi Brojeni AA, Rastin M, Kokhaei P, & Mahmoudi M (2017). Hesperidin ameliorates immunological outcome and reduces neuroinflammation in the mouse model of multiple sclerosis. J Neuroimmunol. 302,23–33. doi: 10.1016/j.jneuroim.2016.11.009 [PubMed: 27912911]

Hanna CB, Yao S, Ramsey CM, Hennebold JD, Zelinski MB, & Jensen JT (2015). Phosphodiesterase 3 (PDE3) inhibition with cilostazol does not block in vivo oocyte maturation in rhesus macaques (Macaca mulatta). Contraception 91,418–22. doi: 10.1016/j.contraception.2015.01.017 [PubMed: 25645461]

Haynes RL & van Leyen K (2013). 12/15-lipoxygenase expression is increased in oligodendrocytes and microglia of periventricular leukomalacia. Dev Neurosci. 35,140–54. doi: 10.1159/000350230 [PubMed: 23838566]

Hertel W, Peschel G, Ozegowski JH, & Müller PJ (2006). Inhibitory effects of triterpenes and flavonoids on the enzymatic activity of hyaluronic acid-splitting enzymes. Arch Pharm (Weinheim) 339,313–8. doi: 10.1002/ardp.200500216 [PubMed: 16718670]

Hunnicutt GR, Primakoff P, & Myles DG (1996). Sperm surface protein PH-20 is bifunctional: one activity is a hyaluronidase and a second, distinct activity is required in secondary sperm-zona binding. Biol Reprod. 55,80–6. [PubMed: 8793062]

Infante JR, Korn RL, Rosen LS, LoRusso P, Dychter SS, Zhu J, Maneval DC, Jiang P, Shepard HM, Frost G, Von Hoff DD, Borad MJ, & Ramanathan RK (2018). Phase 1 trials of PEGylated recombinant human hyaluronidase PH20 in patients with advanced solid tumours. Br J Cancer. 2018 1;118(2):153–161. doi: 10.1038/bjc.2017.327. [PubMed: 28949957]

Jaeger BN, Parylak SL, & Gage FH. (2017). Mechanisms of dietary flavonoid action in neuronal function and neuroinflammation. Mol Aspects Med. Pii, S0098-2997(17)30111-5. doi: 10.1016/j.mam.2017.11.003

Jenkins HG & Bachelard HS (1988). Developmental and age-related changes in rat brain glycosaminoglycans. J. Neurochem. 51, 1634–40. [PubMed: 3139839]

Jiang D, Liang J, Fan J, Yu S, Chen S, Luo Y, Prestwich GD, Mascarenhas MM, Garg HG, Quinn DA, Homer RJ, Goldstein DR, Bucala R, Lee PJ, Medzhitov R, & Noble PW (2005). Regulation of lung injury and repair by Toll-like receptors and hyaluronan. Nat Med. 11, 1173–9. doi: 10.1038/nm1315 [PubMed: 16244651]

Kaessler A, Olgen S, & Jose J (2011). Autodisplay of catalytically active human hyaluronidase hPH-20 and testing of enzyme inhibitors. Eur J Pharm Sci. 42, 138–47. doi: 10.1016/j.ejps.2010.11.004 [PubMed: 21075205]

Khalaj AJ, Hasselmann J, Augello C, Moore S, & Tiwari-Woodruff SK (2016). Nudging oligodendrocyte intrinsic signaling to remyelinate and repair: Estrogen receptor ligand effects. J Steroid Biochem Mol Biol. 160, 43–52. doi: 10.1016/j.jsbmb.2016.01.006 [PubMed: 26776441]

Krasieva TB, Ehren J, O'Sullivan T, Tromberg BJ, & Maher P (2015). Cell and brain tissue imaging of the flavonoid fisetin using label-free two-photon microscopy. Neurochem Int. 89,243–8. doi: 10.1016/j.neuint.2015.08.003 [PubMed: 26271433]

Kuppusamy UR, Khoo HE, & Das NP (1990). Structure-activity studies of flavonoids as inhibitors of hyaluronidase. Biochem Pharmacol. 40, 397–401. [PubMed: 2375774]

Lassmann H (2014). Mechanisms of white matter damage in multiple sclerosis. Glia 62, 1816–30. doi: 10.1002/glia.22597. [PubMed: 24470325]

Lee CW, Seo JY, Choi JW, Lee J, Park JW, Lee JY, Hwang KY, Park YS, & Park YI (2014). Potential anti-osteoporotic activity of low-molecular weight hyaluronan by attenuation of osteoclast cell differentiation and function in vitro. Biochem Biophys Res Commun. 449, 438–43. doi:10.1016/j.bbrc.2014.05.050 [PubMed: 24853804]

Lee HG & Cowman MK. (1994). An agarose gel electrophoretic method for analysis of hyaluronan molecular weight distribution. Anal Biochem. 219, 278–87. doi: 10.1006/abio.1994.1267 [PubMed: 8080084]

Li MW, Yudin AI, VandeVoort CA, Sabeur K, Primakoff P, & Overstreet JW (1997). Inhibition of monkey sperm hyaluronidase activity and heterologous cumulus penetration by flavonoids. Biol Reprod. 56, 1383–9. [PubMed: 9166689]

Li Z, Potts-Kant EN, Garantziotis S, Foster WM, & Hollingsworth JW (2011). Hyaluronan signaling during ozone-induced lung injury requires TLR4, MyD88, and TIRAP. PLoS One 6, e27137. doi: 10.1371/journal.pone.0027137 [PubMed: 22073274]

Liang J, Zhang Y, Xie T, Liu N, Chen H, Geng Y, Kurkciyan A, Mena JM, Stripp BR, Jiang D, & Noble PW (2016). Hyaluronan and TLR4 promote surfactant-protein-C-positive alveolar progenitor cell renewal and prevent severe pulmonary fibrosis in mice. Nat Med. 22, 1285–1293. doi: 10.1038/nm.4192 [PubMed: 27694932]

Lindwall C, Olsson M, Osman AM, Kuhn HG, & Curtis MA (2013). Selective expression of hyaluronan and receptor for hyaluronan mediated motility (Rhamm) in the adult mouse subventricular zone and rostral migratory stream and in ischemic cortex. Brain Res. 1503, 62–77. doi: 10.1016/j.brainres.2013.01.045 [PubMed: 23391595]

Liu S & Cheng C (2017). Akt Signaling Is Sustained by a CD44 Splice Isoform-Mediated Positive Feedback Loop. Cancer Res. 77, 3791–3801. doi: 10.1158/0008-5472.CAN-16-2545 [PubMed: 28533273]

Marella M, Ouyang J, Zombeck J, Zhao C, Huang L, Connor RJ, Phan KB, Jorge MC, Printz MA, Paladini RD, Gelb AB, Huang Z, Frost GI, Sugarman BJ, Steinman L, Wei G, Shepard HM, Maneval DC, & Lapinskas PJ (2017). PH20 is not expressed in murine CNS and oligodendrocyte precursor cells. Ann Clin Transl Neurol. 4, 191–211. doi: 10.1002/acn3.393 [PubMed: 28275653]

Marella M, Jadin L, Keller GA, Sugarman BJ, Frost GI, & Shepard HM (2018). KIAA1199 expression and hyaluronan degradation co-localize in multiple sclerosis lesions. Glycobiology. 28, 958–967. doi: 10.1093/glycob/cwy064. [PubMed: 30007349]

Margolis RU, Margolis RK, Santella R, & Atherton DM (1972). The hyaluronidase of brain. J Neurochem. 19,2325–32. [PubMed: 4658791]

Marques S, Zeisel A, Codeluppi S, van Bruggen D, Mendanha Falcão A, Xiao L, Li H, Häring M, Hochgerner H, Romanov RA, Gyllborg D, Muñoz Manchado A, La Manno G, Lönnerberg P, Floriddia EM, Rezayee F, Ernfors P, Arenas E, Hjerling-Leffler J, Harkany T, Richardson WD, Linnarsson S, & Castelo-Branco G (2016). Oligodendrocyte heterogeneity in the mouse juvenile and adult central nervous system. Science. 352,1326–1329. doi: 10.1126/science.aaf6463 [PubMed: 27284195]

Mi S, Miller RH, Lee X, Scott ML, Shulag-Morskaya S, Shao Z, Chang J, Thill G, Levesque M, Zhang M, Hession C, Sah D, Trapp B, He Z, Jung V, McCoy JM, & Pepinsky RB (2005). LINGO-1 negatively regulates myelination by oligodendrocytes. Nat Neurosci. 8,745–51. doi: 10.1038/nn1460 [PubMed: 15895088]

Mi S, Pepinsky RB, & Cadavid D (2013). Blocking LINGO-1 as a therapy to promote CNS repair: from concept to the clinic. CNS Drugs. 27,493–503. doi: 10.1007/s40263-013-0068-8 [PubMed: 23681979]

Mohamed R, Tarannum S, Yariswamy M, Vivek HK, Siddesha JM, Angaswamy N, & Vishwanath BS (2014). Ascorbic acid 6-palmitate: a potent inhibitor of human and soybean lipoxygenase-dependent lipid peroxidation. J Pharm Pharmacol. 66,769–78. doi: 10.1111/jphp.12200 [PubMed: 24359271]

Pandey AK, Patnaik R, Muresanu DF, Sharma A, & Sharma HS (2012). Quercetin in hypoxia-induced oxidative stress: novel target for neuroprotection. Int Rev Neurobiol. 102,107–46. doi: 10.1016/B978-0-12-386986-9.00005-3 [PubMed: 22748828]

Polansky JR, Toole BP, & Gross J (1974). Brain hyaluronidase: changes in activity during chick development. Science 183,862–4. [PubMed: 4810844]

Preston M, Gong X, Su W, Matsumoto SG, Banine F, Winkler C, Foster S, Xing R, Struve J, Dean J, Baggenstoss B, Weigel PH, Montine TJ, Back SA, & Sherman LS (2013). Digestion products of the PH20 hyaluronidase inhibit remyelination. Ann Neurol. 73, 266–80. doi: 10.1002/ana.23788 [PubMed: 23463525]

Reed MJ, Vernon RB, Damodarasamy M, Chan CK, Wight TN, Bentov I, & Banks WA (2017). Microvasculature of the Mouse Cerebral Cortex Exhibits Increased Accumulation and Synthesis of Hyaluronan With Aging. J Gerontol A Biol Sci Med Sci. 72, 740–746. doi: 10.1093/gerona/glw213 [PubMed: 28482035]

Reitinger S, Laschober GT, Fehrer C, Greiderer B, & Lepperdinger G (2007). Mouse testicular hyaluronidase-like proteins SPAM1 and HYAL5 but not HYALP1 degrade hyaluronan. Biochem J. 401,79–85. doi: 10.1042/BJ20060598 [PubMed: 16925524]

Riehl TE, Santhanam S, Foster L, Ciorba M, & Stenson WF (2015). CD44 and TLR4 mediate hyaluronic acid regulation of Lgr5+ stem cell proliferation, crypt fission, and intestinal growth in postnatal and adult mice. Am J Physiol Gastrointest Liver Physiol. 309, G874–87. doi: 10.1152/ajpgi.00123.2015 [PubMed: 26505972]

Rodney G, Swanson AL, Wheeler LM, Smith GN & Worrel CS (1950). The effect of a series of flavonoids on hyaluronidase and some other related enzymes. J Biol Chem 183,739–747.

Schaffer S & Halliwell B (2012). Do polyphenols enter the brain and does it matter? Some theoretical and practical considerations. Genes Nutr. 7,99–109. doi: 10.1007/s12263-011-0255-5 [PubMed: 22012276]

Scheibner KA, Lutz MA, Boodoo S, Fenton MJ, Powell JD, & Horton MR (2006). Hyaluronan fragments act as an endogenous danger signal by engaging TLR2. J Immunol. 177, 1272–81. [PubMed: 16818787]

Shao Z, Lee X, Huang G, Sheng G, Henderson CE, Louvard D, Sohn J, Pepinsky B, & Mi S (2017). LINGO-1 Regulates Oligodendrocyte Differentiation through the Cytoplasmic Gelsolin Signaling Pathway. J Neurosci. 37,3127–3137. doi: 10.1523/JNEUROSCI.3722-16.2017 [PubMed: 28193690]

Schmitt M, Metzger M, Gradl D, Davidson G, & Orian-Rousseau V (2015). CD44 functions in Wnt signaling by regulating LRP6 localization and activation. Cell Death Differ. 22, 677–89. doi: 10.1038/cdd.2014.156 [PubMed: 25301071]

Sherman LS, Matsumoto S, Su W, Srivastava T, & Back SA (2015). Hyaluronan Synthesis, Catabolism, and Signaling in Neurodegenerative Diseases. Int J Cell Biol. 2015, 368584. doi: 10.1155/2015/368584 [PubMed: 26448752]

Sherman LS & Back SA (2017). Comment on: PH20 is not expressed in murine CNS and oligodendrocyte precursor cells. Ann Clin Transl Neurol. 4, 608–609. doi: 10.1002/acn3.430 [PubMed: 28812051]

Sim GS, Lee BC, Cho HS, Lee JW, Kim JH, Lee DH, Kim JH, Pyo HB, Moon DC, Oh KW, Yun YP, & Hong JT (2007). Structure activity relationship of antioxidative property of flavonoids and inhibitory effect on matrix metalloproteinase activity in UVA-irradiated human dermal fibroblast. Arch Pharm Res. 30, 290–8. [PubMed: 17424933]

Sloane JA, Batt C, Ma Y, Harris ZM, Trapp B, & Vartanian T (2010). Hyaluronan blocks oligodendrocyte progenitor maturation and remyelination through TLR2. Proc Natl Acad Sci U S A. 107, 11555–60. doi: 10.1073/pnas.1006496107 [PubMed: 20534434]

Spagnuolo C, Moccia S, & Russo GL (2017). Anti-inflammatory effects of flavonoids in neurodegenerative disorders. Eur J Med Chem. pii, S0223-5234(17)30683-9. doi: 10.1016/j.ejmech.2017.09.001

Srinivasa V, Sundaram MS, Anusha S, Hemshekhar M, Chandra Nayaka S, Kemparaju K., Basappa, Girish KS, & Rangappa KS (2014). Novel apigenin based small molecule that targets snake venom metalloproteases. PLoS One 9, e106364. doi: 10.1371/journal.pone.0106364 [PubMed: 25184206]

Srivastava T, Diba P, Dean JM, Banine F, Shaver D, Hagen M, Gong X, Su W, Emery B, Marks DL, Harris EN, Baggenstoss B, Weigel PH, Sherman LS, & Back S,A (2018). A TLR/AKT/FoxO3 immune tolerance-like pathway disrupts the repair capacity of oligodendrocyte progenitors. J Clin Invest. 128, 2025–2041. doi: 10.1172/JCI94158. [PubMed: 29664021]

Stangel M, Kuhlmann T, Matthews PM, & Kilpatrick TJ (2017). Achievements and obstacles of remyelinating therapies in multiple sclerosis. Nat Rev Neurol. 13, 742–754. doi: 10.1038/nrneurol.2017.139 [PubMed: 29146953]

Strobl B, Wechselberger C, Beier DR, & Lepperdinger G (1998). Structural organization and chromosomal localization of Hyal2, a gene encoding a lysosomal hyaluronidase. Genomics 53, 214–9. doi: 10.1006/geno.1998.5472 [PubMed: 9790770]

Struve J, Maher PC, Li YQ, Kinney S, Fehlings MG, Kuntz C 4th, Sherman LS (2005). Disruption of the hyaluronan-based extracellular matrix in spinal cord promotes astrocyte proliferation. Glia. 52, 16–24. doi: 10.1002/glia.20215 [PubMed: 15892130]

Su W, Foster SC, Xing R, Feistel K, Olsen RH, Acevedo SF, Raber J, & Sherman LS (2017). CD44 Transmembrane Receptor and Hyaluronan Regulate Adult Hippocampal Neural Stem Cell Quiescence and Differentiation. J Biol Chem. 292, 4434–4445. doi: 10.1074/jbc.M116.774109 [PubMed: 28154169]

Sunabori T, Koike M, Asari A, Oonuki Y, & Uchiyama Y (2016). Suppression of Ischemia-Induced Hippocampal Pyramidal Neuron Death by Hyaluronan Tetrasaccharide through Inhibition of Toll-Like Receptor 2 Signaling Pathway. Am J Pathol. 186,2143–2151. doi: 10.1016/j.ajpath.2016.03.016 [PubMed: 27301359]

Suzuki K, Katzman R, & Korey SR (1965). Chemical Studies on Alzheimer's Disease. J. Neuropathol. Exp. Neurol. 24,211–24. [PubMed: 14280498]

Taylor KR, Yamasaki K, Radek KA, Di Nardo A, Goodarzi H, Golenbock D, Beutler B, & Gallo RL (2007). Recognition of hyaluronan released in sterile injury involves a unique receptor complex dependent on Toll-like receptor 4, CD44, and MD-2. J Biol Chem. 282,18265–75. doi: 10.1074/jbc.M606352200 [PubMed: 17400552]

Termeer C, Benedix F, Sleeman J, Fieber C, Voith U, Ahrens T, Miyake K, Freudenberg M, Galanos C, & Simon JC (2002). Oligosaccharides of Hyaluronan activate dendritic cells via toll-like receptor 4. J Exp Med. 195, 99–111. [PubMed: 11781369]

Triggs-Raine B, Salo TJ, Zhang H, Wicklow BA, & Natowicz MR (1999). Mutations in HYAL1, a member of a tandemly distributed multigene family encoding disparate hyaluronidase activities, cause a newly described lysosomal disorder, mucopolysaccharidosis IX. Proc Natl Acad Sci U S A. 96, 6296–300. [PubMed: 10339581]

Vauzour D (2012). Dietary polyphenols as modulators of brain functions: biological actions and molecular mechanisms underpinning their beneficial effects. Oxid Med Cell Longev. 2012, 914273. doi: 10.1155/2012/914273 [PubMed: 22701758]

Wang WW, Lu L, Bao TH, Zhang HM, Yuan J, Miao W, Wang SF, & Xiao ZC (2016). Scutellarin Alleviates Behavioral Deficits in a Mouse Model of Multiple Sclerosis, Possibly Through Protecting Neural Stem Cells. J Mol Neurosci. 58, 210–20. doi: 10.1007/s12031-015-0660-0 [PubMed: 26514969]

Wang Y, Li M, Xu X, Song M, Tao H, & Bai Y (2012). Green tea epigallocatechin-3-gallate (EGCG) promotes neural progenitor cell proliferation and sonic hedgehog pathway activation during adult hippocampal neurogenesis. Mol Nutr Food Res. 56, 1292–303. doi: 10.1002/mnfr.201200035 [PubMed: 22692966]

Weigel PH & Baggenstoss BA (2017). What is special about 200 kDa hyaluronan that activates hyaluronan receptor signaling? Glycobiology 27, 868–877. doi: 10.1093/glycob/cwx039 [PubMed: 28486620]

Wolf DP, Vandevoort CA, Meyer-Haas GR, Zelinski-Wooten MB, Hess DL, Baughman WL, & Stouffer DL (1989). In vitro fertilization and embryo transfer in the rhesus monkey. Biol. Reprod. 41,335–46. [PubMed: 2508776]

Wolf DP, Thomson JA, Zelinski-Wooten MB, & Stouffer RL (1990). In vitro fertilization-embryo transfer in nonhuman primates: the technique and its applications. Mol. Reprod. Dev. 27,261–80. doi: 10.1002/mrd.1080270313 [PubMed: 2078341]

Xing G, Ren M, & Verma A (2014). Divergent Temporal Expression of Hyaluronan Metabolizing Enzymes and Receptors with Craniotomy vs. Controlled-Cortical Impact Injury in Rat Brain: A Pilot Study. Front Neurol. 5, 173. doi: 10.3389/fneur.2014.00173 [PubMed: 25309501]

Yamamoto H, Tobisawa Y, Inubushi T, Irie F, Ohyama C, & Yamaguchi Y (2017). A mammalian homolog of the zebrafish transmembrane protein 2 (TMEM2) is the long-sought-after cell-surface hyaluronidase. J Biol Chem. 292, 7304–7313. doi: 10.1074/jbc.M116.770149 [PubMed: 28246172]

Yoon S, Chang KT, Cho H, Moon J, Kim JS, Min SH, Koo DB, Lee SR, Kim SH, Park KE, Park YI, & Kim E (2014). Characterization of pig sperm hyaluronidase and improvement of the digestibility of cumulus cell mass by recombinant pSPAM1 hyaluronidase in an in vitro fertilization assay. Anim Reprod Sci. 150, 107–14. doi: 10.1016/j.anireprosci.2014.09.002 [PubMed: 25261076]

Yoshida H, Nagaoka A, Kusaka-Kikushima A, Tobiishi M, Kawabata K, Sayo T, Sakai S, Sugiyama Y, Enomoto H, Okada Y, & Inoue S (2013). KIAA1199, a deafness gene of unknown function, is a new hyaluronan binding protein involved in hyaluronan depolymerization. Proc Natl Acad Sci U S A. 2013 4 2;110(14):5612–7. doi: 10.1073/pnas.1215432110. [PubMed: 23509262]

Yoshino Y, Ishisaka M, Tsuruma K, Shimazawa M, Yoshida H, Inoue S, Shimoda M, Okada Y, & Hara H (2017). Distribution and function of hyaluronan binding protein involved in hyaluronan depolymerization (HYBID, KIAA1199) in the mouse central nervous system. Neuroscience 347, 1–10. doi: 10.1016/j.neuroscience.2017.01.049 [PubMed: 28189611]

Yoshino Y, Goto M, Hara H, & Inoue S (2018). The role and regulation of TMEM2 (transmembrane protein 2) in HYBID (hyaluronan (HA)-binding protein involved in HA depolymerization/KIAA1199/CEMIP)-mediated HA depolymerization in human skin fibroblasts. Biochem Biophys Res Commun. 505, 74–80. doi: 10.1016/j.bbrc.2018.09.097. [PubMed: 30241936]

Yudin AI, Vandevoort CA, Li MW, & Overstreet JW (1999). PH-20 but not acrosin is involved in sperm penetration of the macaque zona pellucida. Mol Reprod Dev. 53, 350–62. doi: 10.1002/(SICI)1098-2795(199907)53:3<350::AID-MRD11>3.0.CO;2-9 [PubMed: 10369396]

Zeng HJ, Ma J, Yang R, Jing Y, & Qu LB (2015). Molecular Interactions of Flavonoids to Hyaluronidase: Insights from Spectroscopic and Molecular Modeling Studies. J Fluoresc. 25, 941–59. doi: 10.1007/s10895-015-1576-3 [PubMed: 26006100]

Zhang Y, Aizenman E, DeFranco DB, & Rosenberg PA (2007). Intracellular zinc release, 12-lipoxygenase activation and MAPK dependent neuronal and oligodendroglial death. Mol Med. 13,350–5. doi: 10.2119/2007-00042.Zhang [PubMed: 17622306]

Zhu R, Huang YH, Tao Y, Wang SC, Sun C.h., Piao HL, Wang XQ, Du MR, & Li DJ (2013). Hyaluronan up-regulates growth and invasion of trophoblasts in an autocrine manner via PI3K/AKT and MAPK/ERK1/2 pathways in early human pregnancy. Placenta 34,784–91. doi: 10.1016/j.placenta.2013.05.009 [PubMed: 23806178]

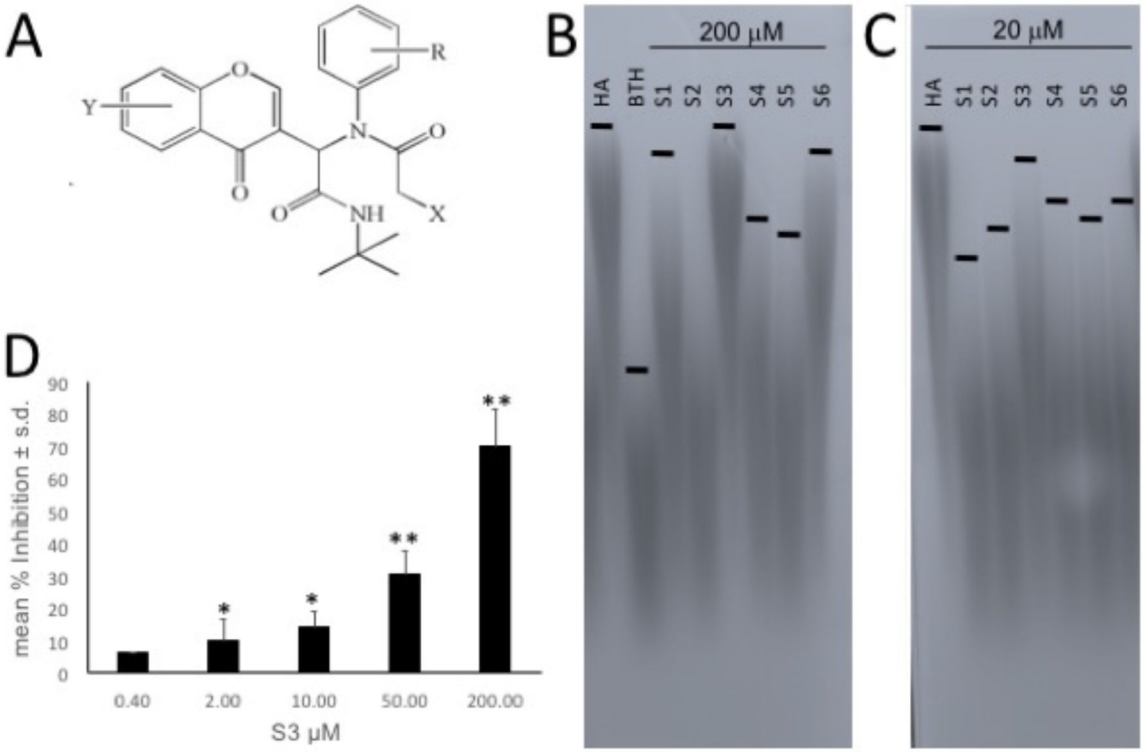

Figure 1:

Modified flavonoids with distinct structures inhibit the activity of bovine testicular hyaluronidase. (A) Varieties of chemical structures resulting from synthesis of modified flavonoids. (B) Agarose gel of preparations of HMW HA either untreated (“HA”), treated with bovine testicular hyaluronidase (“BTH”), or BTH with 200 μM of each modified flavonoid (S1-S6) stained with Stains-All. (C) Agarose gel of preparations of HMW HA as in B but with 20 μM of each modified flavonoid. (D) Quantification of mean % BTH inhibition by S3 at different concentrations. *p<0.001; **p<0.0001

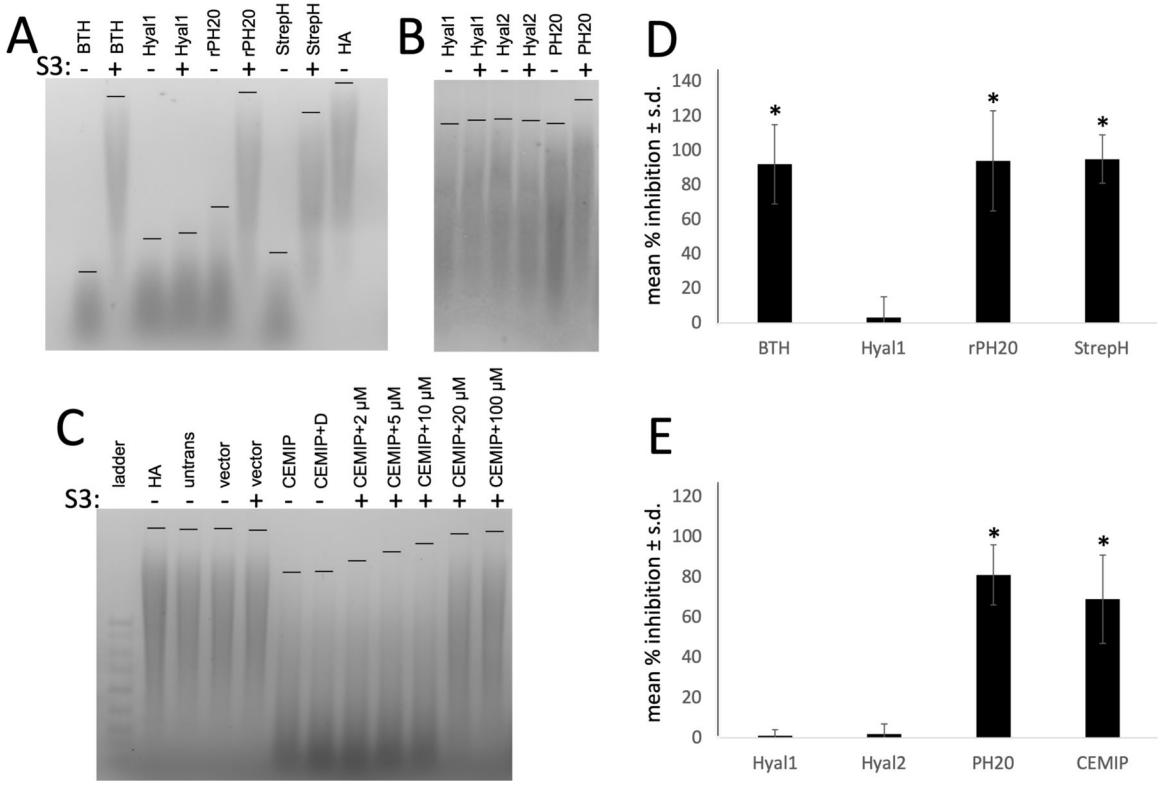

Figure 2:

Effects of the S3 flavonoid on the activities of different hyaluronidases. (A) Effects of 20 µM S3 ("+") on HA digestion by BTH, recombinant Hyal1, recombinant PH20 (rPH20), and *Streptomyces* hyaluronidase compared to enzymes treated with vehicle alone ("-"). The "HA" lane was incubated without S3 but with the vehicle from the hyaluronidases. (B) Effects of the S3 flavonoid on HA digestion by lysates from HEK-293 cells transfected with empty vector ("vector") or cells transfected with Hyal1, Hyal2, or PH20 compared to HA digested by rPH20 or BTH or to undigested HA "HA". (C) Effects of different concentrations of S3 or vehicle alone (DMSO - "D") on HA digestion by HEK-293 cells either untransfected ("untrans"), transfected with vector alone, or transfected with an expression vector carrying the cDNA for *Cemip*. (D) Quantification of the inhibition of HA digestion by S3 (20 µM) in the presence of recombinant Hyal1, recombinant PH20, BTH, or *Streptomyces* hyaluronidase. *p<0.01. (E) Quantification of HA digestion in live cell cultures of HEK-293 cells treated with S3 (20 µM) following transfection with either *Hyal1*, *Hyal2*, *PH20* or *Cemip* expression vectors. *p<0.005.

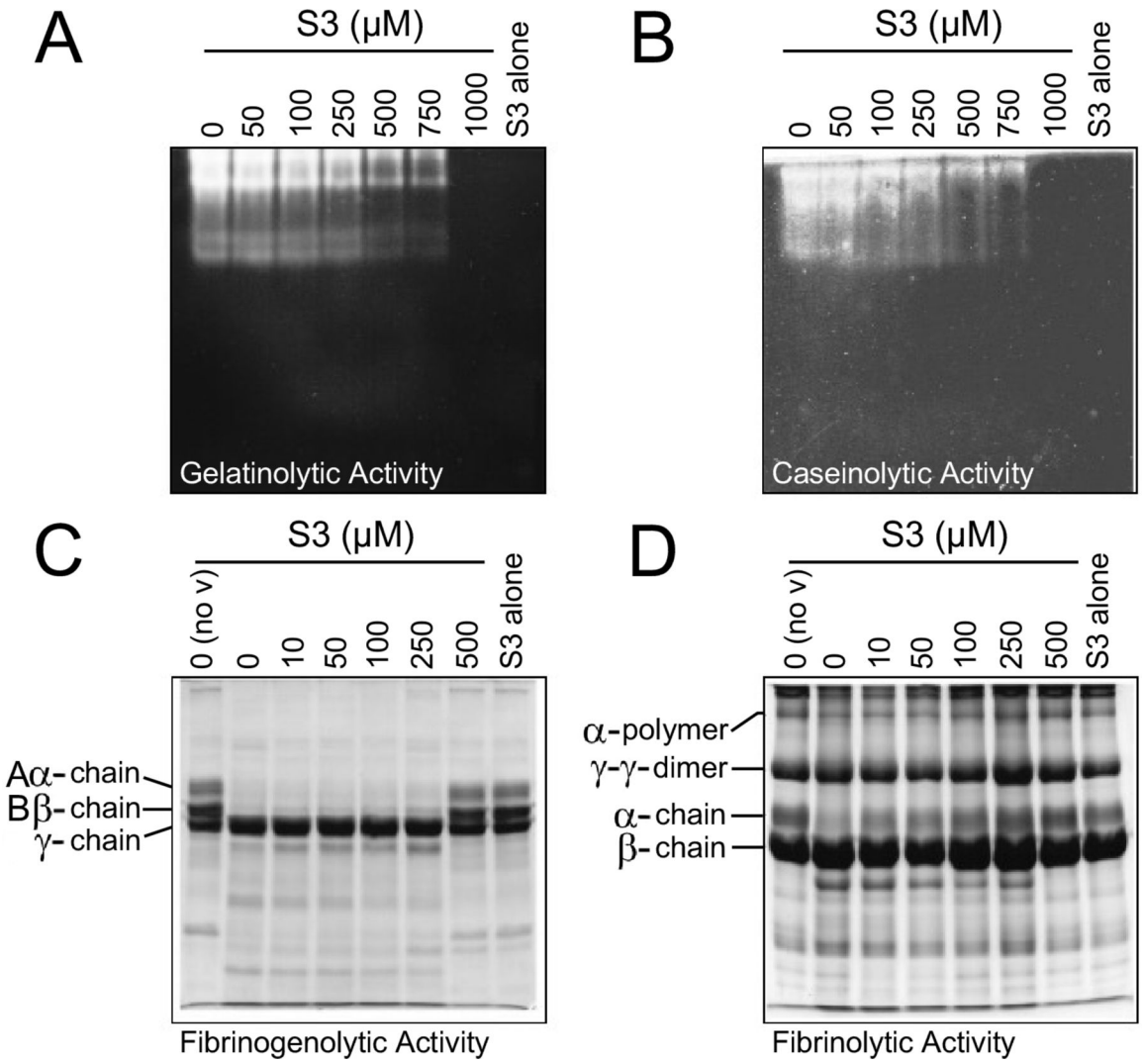

Figure 3:

Effects of S3 on proteolytic and fibrin(ogen)olytic activity of *Echis carinatus* venom. Zymograms showing (A) gelatinolytic activity and (B) caseinolytic activity of *Echis carinatus* venom. The venom (3 μg) was pre-incubated (10 min at 37°C) with different concentrations of S3 as shown in 50 μl reaction mixture. The "S3 alone" lane represents S3 (1000 μM) alone as a negative control. Samples were electrophoresed on gels impregnated separately with gelatin (1%) and casein (0.2%) as substrate. (C) Gels showing Fibrinogenolytic activity and (D) Fibrinolytic activity of *Echis carinatus* venom. The venom (0.2 μg) was pre-incubated (10 min at 37°C) with different concentrations of S3 as shown and the lytic activity of the venom was initiated by adding respective substrates; fibrinogen (50 μg) and fibrin clot incubated for 30 min in 40 μl reaction mixture. The "0 (no v)" lane represents substrate alone and "S3 alone" lane represents substrate with S3 (500 μM). Samples were electrophoresed and processed according to the standard protocol.

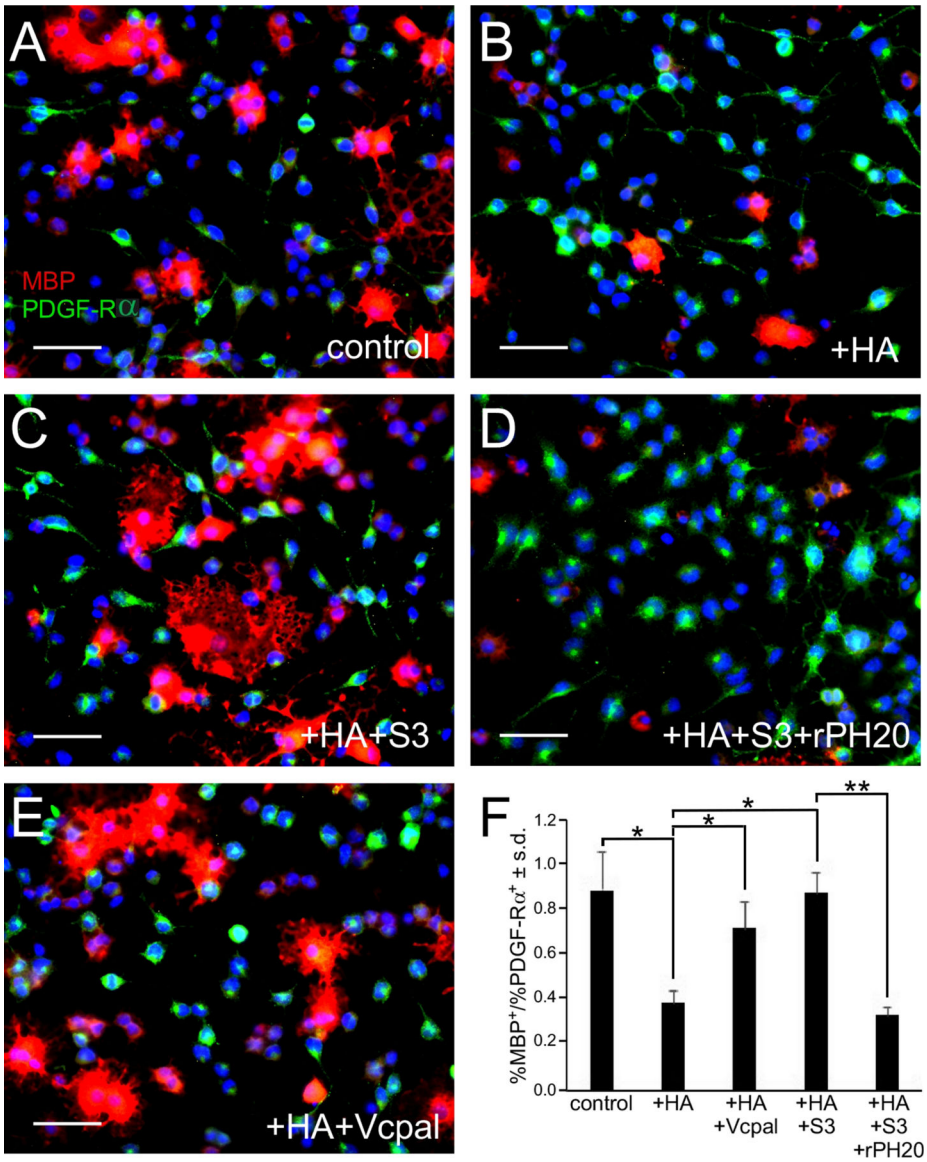

Figure 4:

Effects of blocking hyaluronidase activity on HA-mediated inhibition of OPC maturation. (A) Mouse OPCs grown under conditions that favor maturation in the absence of HA. (B) OPCs grown as in A in the presence of HMW HA. (C) OPCs grown as in B in the presence of 2 μM S3. (D) OPCs grown as in C in the presence of 25 U rPH20. (E) OPCs grown as in B in the presence of 25 μM Vcpal. Red = MBP; green = PDGFRα. Scale bars = 50 μm. (F) Quantification of the results in A-E. c = vehicle control; vc = Vcpal; P = PH20. Note that the data to the right of the dashed lines was from a separate experiment where HA was not added to the cultures. *$p<0.001$; **$p<0.0005$

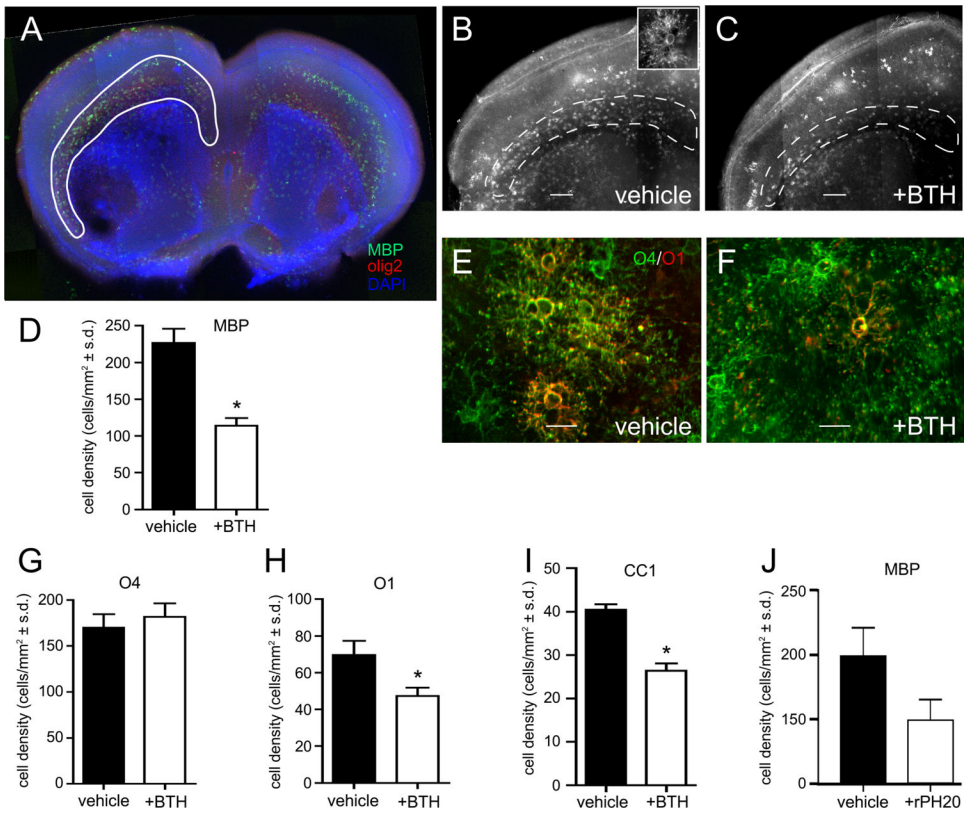

Figure 5:

Bovine testicular hyaluronidase and rPH20 block OPC maturation in a model of perinatal white matter injury. (A) Montage of low magnification images of a brain slice including the corpus callosum (outlined) stained with DAPI (blue), MBP (green), and olig2 (red), demonstrating the area where slices were analyzed for changes in OPC maturation. (B) A representative slice treated with vehicle and stained for MBP (white). Inset in B: high magnification image from the same slice, showing the morphology of a maturing oligodendrocyte. (C) A representative slice treated with 20 U/ml BTH and stained for MBP (white). Scale bars = 500 μm. Dotted lines outline the corpus callosum. (D) Quantification of MBP labeling in slices treated with vehicle or BTH. (E) Immunostaining of O4 (green) and O1 (red) from a representative slice treated with vehicle. (F) Immunostaining for O4 and O1 from a representative slice treated with 20 U/ml BTH. Scale bars = 20 μm. (G-I) Quantification of immunostaining in slice cultures for O4 (G), O1 (H) and CC1 (I). (J) Quantification of immunostaining from slices treated with vehicle or 20 U/ml of rPH20. For the MBP experiments, sham = 6 animals; hyaluronidase = 5 animals (both from 3 independent culture days). We analyzed ~3 slices from each animal (some removed because of poor viability), with a total of 10 slices in the PBS control and 12 slices in the hyaluronidase group. For the O4/O1 experiments, sham = 4 animals; hyaluronidase = 5 animals (both from 3 independent culture days). We used a total of 15 slices in the control group, and 15 slices in the hyaluronidase group. Comparisons were analyzed using a Student's t-test. *$p<0.001$.

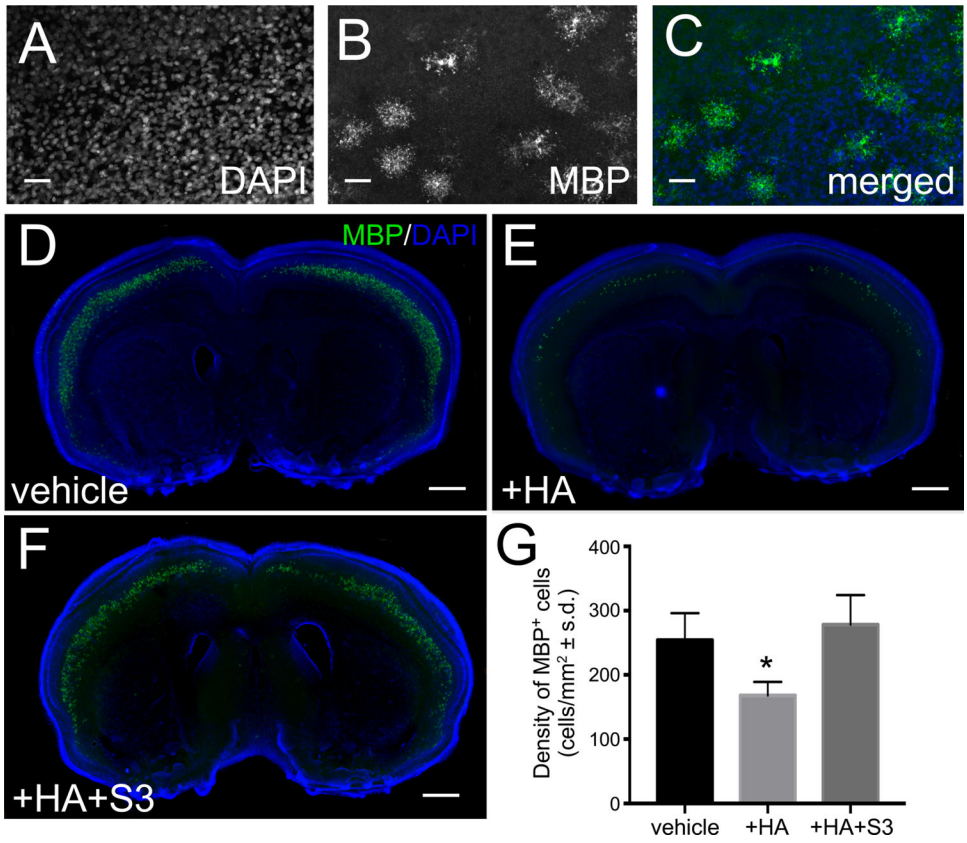

Figure 6:

Effects of blocking hyaluronidase activity on OPC maturation in a model of perinatal white matter injury. (A-C) Examples of typical MBP staining and cell morphology used for quantification of mature cells. Cells were stained for DAPI (A) and MBP (B), and images were merged (C) with DAPI in blue and MBP in green. (D) Slice treated with vehicle. (E) Slice treated with (100 μg/ml) HMW HA. (F) Slice treated with HMW HA and 2 μM S3. Images shown are from one representative experiment. (G) Quantification of MBP+ cells in slices. Note that data to the right of the dashed line was from a separate experiment in which HA was not added to the cultures. Green = MBP; blue = DAPI to stain cell nuclei. Cells were counted in the corpus callosum (the whole corpus callosum using the meander scan function of Stereo-Investigator at 20x magnification). Scale bars = 500 μm. *$p<0.001$, n=3 (e.g. means from 3 separate experiments using 3 slices per condition prepared from 3 separate litters).

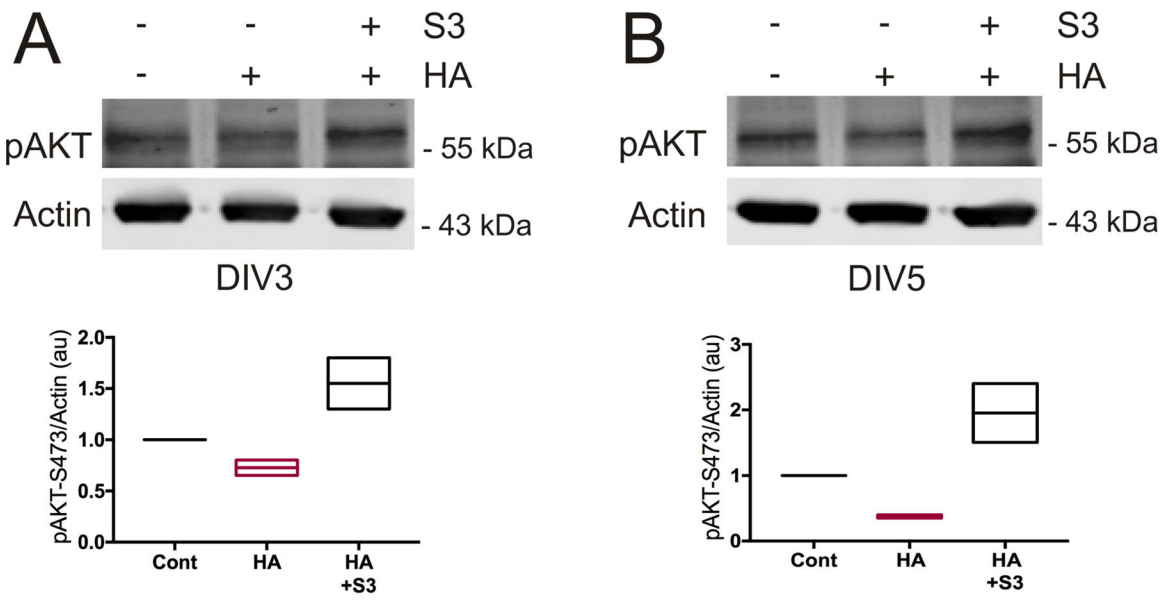

Figure 7:

S3 reverses the effects of HMW HA on AKT phosphorylation. (A-B) Persistent AKT de-phosphorylation in rat slices treated with HMW HA (100ug/ml). Representative blots (upper panels) and quantification (lower panels) probed with pAKT-S473 and Actin antibodies. Note that co-treatment with S3 (2 μM) promoted an increase in AKT phosphorylation to levels even higher than PBS treated controls at 3 days (A) and 5 days (B). A-B: n=2 independent studies from 2 separate litters; 2 slices/condition.

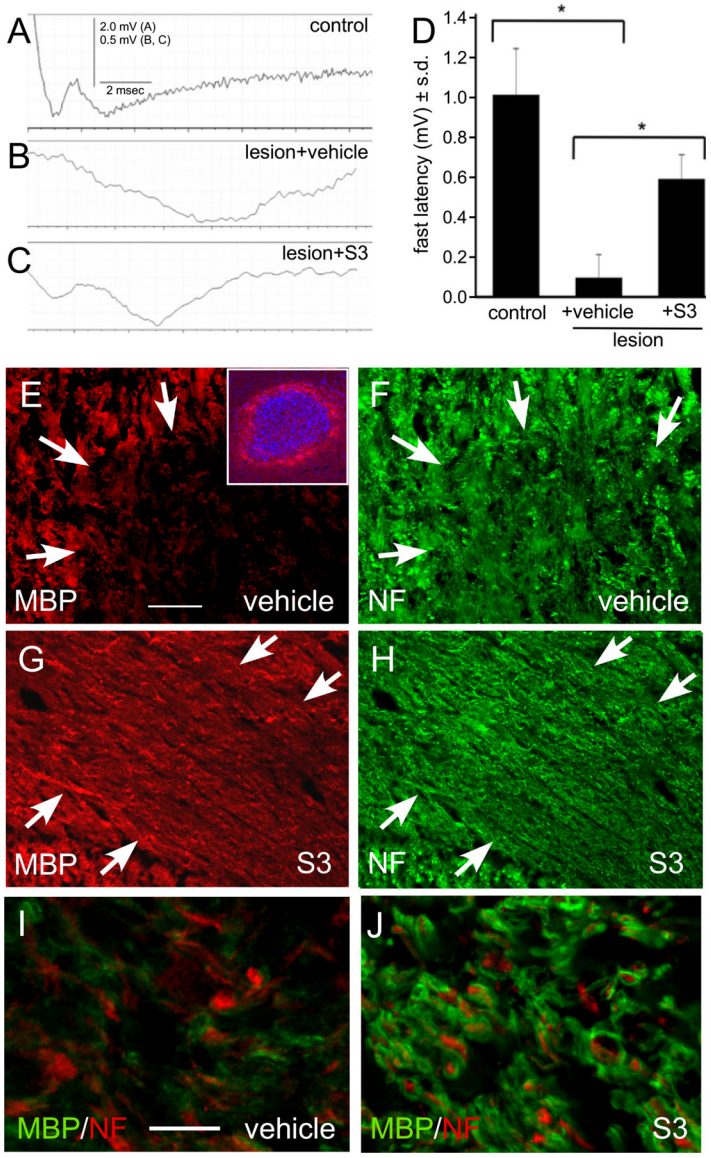

Figure 8:

Blocking hyaluronidase activity promotes functional remyelination. (A-C) Representative compound action potential (CAP) recordings of slices from (A) Sham control; (B) lysolecithin corpus callosum lesions treated with vehicle; and (C) lysolecithin corpus callosum lesions treated with S3. (D) Quantification of CAP recordings. *p<0.001. The N1/N2 peaks are clearly visible in traces A and C. In panel B, our interpretation is that the response consists of a mixed population of unmyelinated, partially myelinated and myelinated fibers, producing a broad CAP response that lacks discrete subpopulations. (E-H) Immunohistochemical staining of slices following CAP recordings from (E, F) animals treated with vehicle and (G, H) animals treated with S3. Red = MBP (E, G); green = neurofilament (NF). Scale bars = 20 μm. (I) Confocal images of lesion treated with vehicle as in (B). (J) Confocal images of lesion treated with S3 as in (C). Scale bars = 4 μm.

Table 1:

Effects of S3 on *in vitro* fertilization rates

Treatment	% Fertilized (2 μM S3)	% Fertilized (20 μM S3)
Vehicle Oocyte + Vehicle Sperm	94	46
Vehicle Oocyte + S3 Sperm	64	0.1
S3 Oocyte + Vehicle Sperm	67	0.1
S3 Oocyte + S3 Sperm	70	0.1